E-cadherin Controls Bronchiolar Progenitor Cells and Onset of Preneoplastic Lesions in Mice[1,2]

Fatih Ceteci[*,3], Semra Ceteci[*], Emanuele Zanucco[*], Chitra Thakur[*], Matthias Becker[†], Nefertiti El-Nikhely[‡], Ludger Fink[§], Werner Seeger[‡], Rajkumar Savai[‡] and Ulf R. Rapp[*,‡]

*Department of Molecular Biology, Max Planck Institute of Biochemistry, Martinsried, Germany; †Institut für Medizinische Strahlenkunde und Zellforschung (MSZ), University of Würzburg, Würzburg, Germany; ‡Department of Lung Development and Remodeling, Max Planck Institute for Heart and Lung Research, Bad Nauheim, Germany; §Department of Pathology, University of Giessen Lung Center, Giessen, Germany

Abstract

Although progenitor cells of the conducting airway have been spatially localized and some insights have been gained regarding their molecular phenotype, relatively little is known about the mechanisms regulating their maintenance, activation, and differentiation. This study investigates the potential roles of E-cadherin in mouse Clara cells, as these cells were shown to represent the progenitor/stem cells of the conducting airways and have been implicated as the cell of origin of human non–small cell lung cancer. Postnatal inactivation of E-cadherin affected Clara cell differentiation and compromised airway regeneration under injury conditions. In steady-state adult lung, overexpression of the dominant negative E-cadherin led to an expansion of the bronchiolar stem cells and decreased differentiation concomitant with canonical Wnt signaling activation. Expansion of the bronchiolar stem cell pool was associated with an incessant proliferation of neuroepithelial body–associated Clara cells that ultimately gave rise to bronchiolar hyperplasia. Despite progressive hyperplasia, only a minority of the mice developed pulmonary solid tumors, suggesting that the loss of E-cadherin function leads to tumor formation when additional mutations are sustained. The present study reveals that E-cadherin plays a critical role in the regulation of proliferation and homeostasis of the epithelial cells lining the conducting airways.

Neoplasia (2012) 14, 1164–1177

Introduction

Lung morphogenesis commences with the outgrowth of an endodermally derived lung primordium that eventually forms the primitive trachea and bronchi. In response to signals from the mesenchyme, the primitive bronchi undergo repetitive rounds of budding and stereotypic branching to form the architecture of the lung. During this process, differentiation of distinct respiratory epithelial cell types occurs progressively in the perinatal and postnatal periods, producing the various cells lining the conducting (basal, ciliated, Clara, and neuroendocrine cells) and peripheral (alveolar type I and type II cells) airways. Cell differentiation during lung morphogenesis is regulated by many factors including Wnt, Fgf, Shh, and BMP signaling [1].

After lung development, respiratory epithelium undergoes slow homeostatic turnover resulting in the replacement of much of the epithelium after 4 months in rodents [2]. Despite low cell turnover, the respiratory epithelium is capable of extensive proliferation following injury [3–7]. Cell type–specific injury models have identified several

putative stem/progenitor cells residing in discrete niches along the proximal-distal axis of the airways [7,8]. The endogenous stem cell pools in normal adults usually respond to injury and starts tissue repair. However, as adult stem cells are not immortal, this process is limited and regeneration is incomplete. Besides, to aid a rapid repair, alveolar epithelial cells (AECs) act as progenitor cells upregulating a stem/progenitor cell marker during the recovery phase. This suggests that either AECs contain a subpopulation of progenitor cells or the majority of AECs can undergo reactivation into a progenitor-like state in response to injury [9].

Clara cells represent an abundant population of long-term progenitors that contribute to bronchiolar repair following injury to ciliated cells [10–13]. Within the normal lung, Clara cells maintain a progenitor cell pool that needs to be stabilized for the sake of tissue repair in case of injury. Clara cells can also undergo metaplasia to mucous-producing cells restoring terminally differentiated cells of the conducting airway epithelium [14]. Dose-dependent depletion of the Clara cells in mice by naphthalene exposure revealed activation of rare pollutant-resistant Clara cells [variant Clara (Clara^V)] that were localized to the neuroepithelial body (NEB) and at the bronchoalveolar duct junction (BADJ) [7,15,16]. Another subset of Clara cells that proliferate following lung injury are bronchoalveolar stem cells (BASCs). These cells are located at the BADJ microenvironment and were initially identified by their co-expression of Scgb1a1 (marker of Clara cells) and surfactant protein C (Sftpc) (alveolar type II cell marker) [17]. When sorting these cells by flow cytometry (as Sca11, CD341 cells), they can both self-renew *in vitro* and give rise to bronchiolar and alveolar cell types. Furthermore, these cells are a target of activated Ras-mediated neoplastic transformation in the mouse. More recently, deletion of p38 mitogen-activated protein (MAP) kinase in the adult lung was shown to cause increased levels of proliferation in the alveoli at steady state, to cause an increase in the number of dual-positive (CCSP1, SpC1) cells, and to make the lung more susceptible to activated Ras-mediated oncogenic transformation (45). Even though stem cells of the conducting airway have been spatially localized and some insights have been gained regarding their molecular phenotype, relatively little is known about the mechanisms regulating their maintenance, activation, and differentiation.

E-cadherin is a major component of adherens junctions between epithelial cells and plays a pivotal role in epithelial differentiation during embryonic development [18]. E-cadherin–deficient mice die very early after the morula stage due to impaired trophectoderm formation [19,20]. Tissue-specific ablation of E-cadherin in hair follicles or skin of mice resulted in altered epidermal differentiation [21,22], whereas in mammary glands impaired terminal differentiation was observed after abrogation of E-cadherin expression [23]. In the lung, inhibiting the ability of E-cadherin to form intercellular junctions in lung primordial explants has been shown to impair lung branching morphogenesis [24]. We have recently demonstrated that disruption of E-cadherin in mature alveolar type II cells leads to diffuse hyperplasia and alveolar space enlargement [25]. These studies point to a role for E-cadherin in lung epithelial differentiation and homeostasis in the adult airways. In addition to its fundamental role in tissue morphogenesis, E-cadherin is frequently implicated in several types of human cancer. Loss of E-cadherin has been commonly associated with tumor progression by promoting invasive growth, angiogenesis, metastatic dissemination, and colonization of tumor cells [25–27].

Hence, the aim of this study is to determine the function of E-cadherin in differentiation and maintenance of the conducting airway epithelium by disrupting E-cadherin function in mouse Clara cells

in the adult lung. In addition, we also aimed to determine whether disruption of E-cadherin in Scgb1a1-expressing cells causes lung cancer.

Materials and Methods
For details of the experimental setup, see Supplementary Materials and Methods.

Mouse Strains
Scgb1a1 rtTA mice were maintained on FVB/n background. *Tet-O dn E-cadherin* transgenic mice were maintained on C57Bl/6 background. These transgenic mice have a truncated *E-cadherin* gene where most of the extracellular domain of mouse E-cadherin was excised. The transgene was preceded by a c-myc epitope and will be referred to as dn E-cadherin [28]. Compound mice were induced with doxycycline (DOX) containing food for different periods and analyzed for the phenotypic accuracy of lung pathology. All animal experiments were performed according to the regulations of the Bavarian State authorities.

RNA Isolation and Reverse Transcription–Polymerase Chain Reaction Analysis
Total RNA was isolated from whole lungs of mice, followed by First-Strand c-DNA Synthesis Kit. Real-time reverse transcription–polymerase chain reaction (RT-PCR) was performed using the DyNAmo HS SYBR Green qPCR Kit in a Roto-Gene 2000 Detection System with previously described primers [29–31].

Immunoblot Analysis
Protein was extracted from left lung lobes of mice. Immunoblot analysis was performed using the following antibodies: myc tag and actin.

Histopathology and Immunostainings
Immunohistochemistry and immunofluorescent staining were performed on mouse lung paraffin sections using the following antibodies: CYP2F2, Scgb1a1, Ki67, pro Sftpc, vimentin, E-cadherin, phospho-Akt, phospho-ERK, activated β-catenin, myc tag, acetylated tubulin, PGP 9.5, and β-catenin. For microscopy, we employed the Zeiss Axio Scope.A1 or the Zeiss Discovery.V8 Stereo microscopes (Carl Zeiss MicroImaging GmbH, Göttingen, Germany) integrated with an Axio-Cam ICc3 camera (Spectra Service, Ontario, NY). Images were acquired using AxioVision Rel. 4.7 software provided by Zeiss. Negative controls included the omission of the primary antibody.

Morphometric Analysis
Quantitation of ciliated cells was assessed by determining the length of basement membrane underlying tubulin$^+$ regions of the epithelium and dividing this value by the total length of the basement membrane. Ciliated cells were scored from at least 10 bronchioles per lung. Epithelial repair was quantified at day 2 and day 18 of treatment recovery by determining the length of basement membrane underlying CYP2F2$^+$ or Scgb1a1$^+$ regions of the epithelium and dividing this value by the total length of the basement membrane. The length of the bronchial epithelium was determined using the measurement function of Zeiss Axio Scope.A1. For quantitative assessment of NEB-associated pulmonary neuroendocrine cells (PNECs) or Clara^V cell proliferation, triple immunofluorescence staining was performed on lung sections using CGRP, Scgb1a1, and Ki-67 antibodies. Clara^V

cells were identified with their association with CGRP-expressing neighboring NE cells.

Naphthalene Exposure

Five-week-old male compound (*Scgb1a1 rtTA/Tet-O dn E-cadherin*) mice were intraperitoneally injected with 250 mg/kg body weight of naphthalene (Sigma, Munich, Germany) dissolved in corn oil. Animals were sacrificed 2 or 18 days following naphthalene or corn oil treatments.

BASC Sorting by Flow Cytometry

BASCs were isolated from the lungs of 6-week-old double-transgenic (DTR) mice according to established protocols [17]. Isolated cells were sorted using FACSCalibur (BD Immunocytometry Systems, Heidelberg, Germany) according to the manufacturer's instructions.

Statistical Analysis

All statistical analyses were performed using GraphPad Prism 5 software (GraphPad Software, Inc, San Diego, CA). Student's *t* test (two-tailed) was used to compare two groups. When more than two groups were compared, differences among the groups were determined by one-way analysis of variance. Differences between means were considered statistically significant when $P < .05$.

Results

E-cadherin Is Necessary for Clara Cell Differentiation in Steady-state Adult Lung

To determine the potential role of E-cadherin in murine lung non-ciliated secretory epithelial cells (Clara cells), DTR mice were generated by crossing *Scgb1a1-rtTA* mice with mice expressing a myc-tagged dominant negative mutant of E-cadherin under the control of a DOX-regulatable promoter (*Tet-O* dn E-cadherin–myc tag mice; Figure 1*A*). The resulting compound mice were either untreated or treated with DOX. Lung lysates obtained from adult DTR mice showed expression of myc-tagged dn E-cadherin after 1 week DOX administration in both the conducting and the alveolar portion of
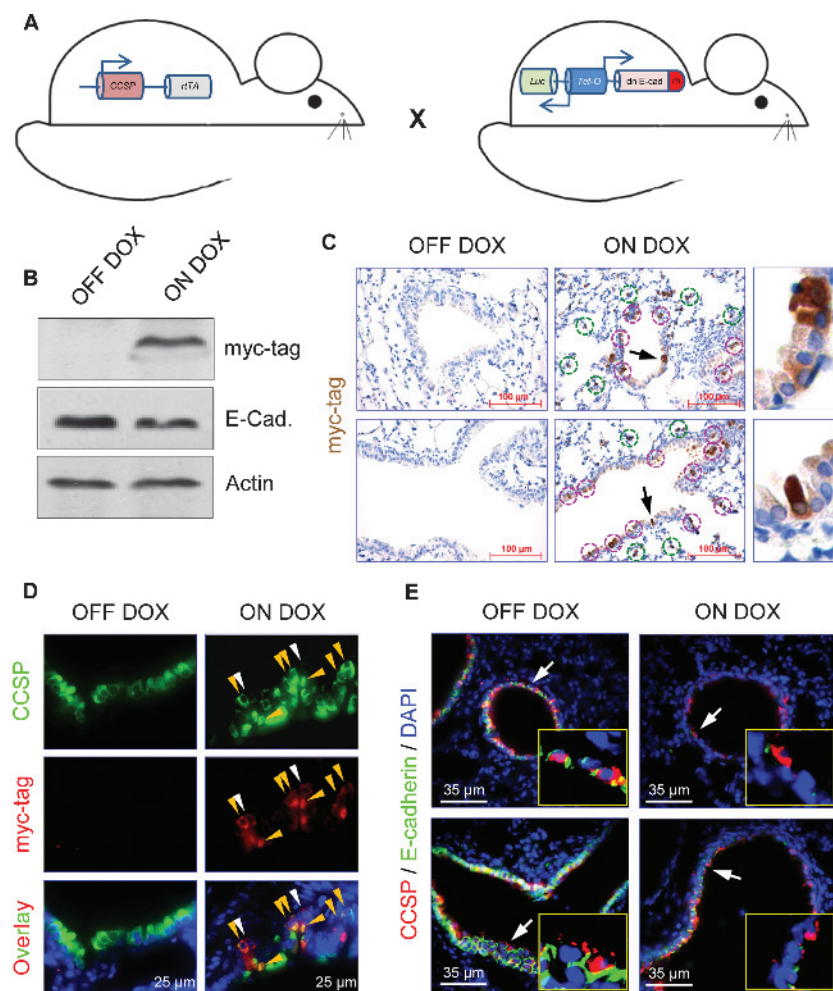
Figure 1. Conditional inactivation of E-cadherin in steady-state lungs alters Clara cell differentiation. (A) Construct and breeding strategy used to inactivate E-cadherin in Clara cells in the conducting airway. m, myc tag. (B) Immunoblot analysis shows transgene expression only in the presence of DOX. Actin was used as a control. (C) Immunohistochemical staining of lung sections for myc tag. Five-week-old DTR mice were either untreated (OFF DOX) or DOX-treated (ON DOX) for 1 week before analysis. Transgene expression was detected both in conducting airways (red circles) and in the alveoli (green circles). Arrows in C indicate regions shown in insets. Hematoxylin (blue) was used as a counterstain. Scgb1a1/myc tag (D) and Scgb1a1/E-cadherin (E) dual immunofluorescence stainings of lung sections from control and induced adult mice. Myc tag–expressing Clara cells are shown with orange arrows. White arrows in D show Scgb1a1-negative but myc tag–positive cells. Arrows in E indicate regions shown in insets. Nuclei were counterstained with 4′,6-diamidino-2-phenylindole (DAPI, blue).

the airways after induction (Figure 1, B and C). Furthermore, we observed reduced endogenous E-cadherin level (Figure 1B) and lack of endogenous E-cadherin expression in dn E-cadherin–expressing conducting airway cells after induction (Figure W1). To show the specific localization of dn E-cadherin expression in Clara cells, dual immunofluorescence staining using myc tag and Scgb1a1 antibodies was performed. In accordance with the activity of rat *Scgb1a1* promoter in adult lung [12], subsets of Clara cells were found to express myc-tagged dn E-cadherin after induction (Figure 1D). Notably, we found that some Clara cells that were negative for Scgb1a1 in conducting airway epithelium stained positive for myc tag, suggesting that the inactivation of E-cadherin alters Clara cell differentiation (Figure 1D). This decrease in Scgb1a1 expression paralleled with the remarkable loss of E-cadherin in both small and large conducting airways of the DOX-treated mice (Figure 1E).

To further evaluate the effect of loss of E-cadherin function on bronchiolar epithelial cell differentiation, we have performed immunofluorescence staining of ciliated cells using tubulin antibody that recognizes ciliated cells. Induction of dn E-cadherin in respiratory epithelium of the DOX-treated animals caused a significant decrease in the number of ciliated cells (Figure 2, A and B). Analysis of three secretory cell–specific mRNAs, Scgb1a1, CYP2F2, and FoxJ1 (a ciliated cell marker), by quantitative RT-PCR supported the results of the immunofluorescence stainings and showed significantly lower mRNA abundance in DOX-treated mice at all ages analyzed (Figure 2C), whereas the abundance of pro Sftpc mRNA, a marker for early lung epithelial progenitor cells and alveolar type II cells, or Aquaporin-5 mRNA, a marker for alveolar type I epithelial cells, did not vary between DOX-treated and untreated DTR mice (Figure 2C). However, after DOX treatment, we observed ectopic pro Sftpc expression within a small fraction of conducting airways, a region of the lung where alveolar type II cells are normally not found (Figure 2, D and E). Taken together, these data demonstrate that overexpression of mutant E-cadherin leads to defective Clara cell epithelial differentiation and ectopic expression of pro Sftpc in conducting airway epithelium.

Overexpression of dn E-cadherin in Clara Cells Attenuates Epithelial Reparative Capacity in the Bronchioles

To determine whether signaling by E-cadherin is necessary for the regeneration of conducting airway epithelium, 5-week-old DTR mice were exposed to naphthalene, which causes site-selective injury to mouse bronchiolar Clara cells [32], followed by a recovery phase of 2 and 18 days, respectively, in the presence or absence of DOX. Consistent with earlier reports, conducting airway epithelium of DTR mice treated with a single dose of naphthalene showed almost no Scgb1a1 immunoreactivity 2 days after injury compared to corn oil–treated DTR mice (Figure 3A). Clusters of naphthalene-resistant and cycling Scgb1a1-expressing cells that have been previously shown to serve as regenerative foci [12] are maintained in the conducting airways (Figure 3B). Notably, despite severe loss of Scgb1a1 expression, naphthalene treatment alone did not affect E-cadherin expression in the conducting airways 2 days after injury in contrast to bronchioles of DTR mice that were treated both with naphthalene and DOX simultaneously (Figure W2).

To analyze whether naphthalene-resistant cells of the bronchioles are capable of appropriate epithelial renewal, conducting airways of DTR mice were compared 18 days after administration of naphthalene or corn oil. Efficacy of epithelial renewal within bronchioles was determined by counting CYP2F2 (Clara cell–specific marker) and Scgb1a1-

immunoreactive cells in untreated and naphthalene-treated animals. As expected, no significant differences in the abundance of CYP2F2-immunoreactive cells between corn oil and naphthalene-exposed groups were observed (Figure 3, C and D). A dramatic reduction in CYP2F2-immunoreactive cells was observed in the bronchioles of DTR mice that were exposed to both naphthalene and DOX (Figure 3, C and D) simultaneously. Similar data were obtained when Scgb1a1-positive cells were scored (Figure 3E). The CYP2F2-positive cells within the bronchioles of naphthalene and DOX mice were also qualitatively different. Instead of uniform expression as observed in corn oil– or naphthalene-only–treated mice, E-cadherin–deficient bronchioles generally showed low level of CYP2F2 expression (Figure 3C). The low-level expression of CYP2F2 observed in these mice may reflect abnormal development of Clara cells repopulating the airways due to disruption in bronchiolar stem cells and differentiation. Alternatively, reduction of CYP2F2 staining in naphthalene-treated E-cadherin–deficient bronchioles (naphthalene and DOX) may arise from altered differentiation of Clara cells (Figure 1D) rather than an impairment of Clara cell regeneration. We therefore compared the level of CYP2F2-expressing cells in DOX-induced DTR mice in the presence or absence of naphthalene. Although there was a reduction in CYP2F2-positive cells as early as 2 days after DOX treatment (Figure 3C), the inhibition of Clara cell regeneration was much less severe than in naphthalene and DOX–exposed animals (Figure 3, D and E). Notably, prolonged DOX treatment in the absence of naphthalene exposure not only generated conducting airways with low CYP2F2-expressing Clara cells but also led to their expansion compared to other groups (Figure 3C). These data demonstrate that expression of dn E-cadherin in Scgb1a1-expressing cells affects restoration and differentiation of bronchiolar epithelium after depletion of the Clara cell population.

Disruption of E-cadherin in Steady-state Adult Lungs Results in an Abnormal Maintenance of Epithelial Cell Populations in Multiple Progenitor Cell Niches

To determine whether the epithelial restoration defects arising from loss of E-cadherin expression in conducting epithelium is associated with abnormal maintenance of bronchiolar lung stem cells, we monitored proliferation of Clara^V and PNE cells following naphthalene-induced lung injury. As reported previously, acute Clara cell depletion caused significant proliferation of Clara^V and PNE cells 2 days after naphthalene exposure compared to the control group (Figure 4, A–C). Consistent with restored bronchiolar epithelium, there was no discernable cell proliferation 18 days after recovery (Figure 4, A–C). Despite impaired epithelial renewal (Figure 3, D and E), comparable proliferation rates of Clara^V and PNE cells were found in mutant E-cadherin–expressing conducting airways after naphthalene-induced lung injury (Figure 4, A–C). Interestingly, treatment of DTR mice with DOX for 2 days also resulted in proliferation of Clara^V and PNE cells in the absence of naphthalene treatment (Figure 4, A–C). Moreover, in contrast to naphthalene-exposed animals, both Clara^V and PNE cells continued to proliferate after prolongation of DOX treatment for 18 days (Figure 4, A–C).

Another putative stem cell niche that was also found to be resistant to naphthalene-induced toxicity is the BASCs [17]. The ectopic pro Sftpc expression in the conducting airway epithelium (Figure 2D) suggested that either the proximal-distal airway patterning was disrupted or the number of specific cell types expressing pro Sftpc in the conducting airway epithelium was increased. Loss of Scgb1a1 expression in the alveolar epithelium argues against a simple loss of proximal-distal
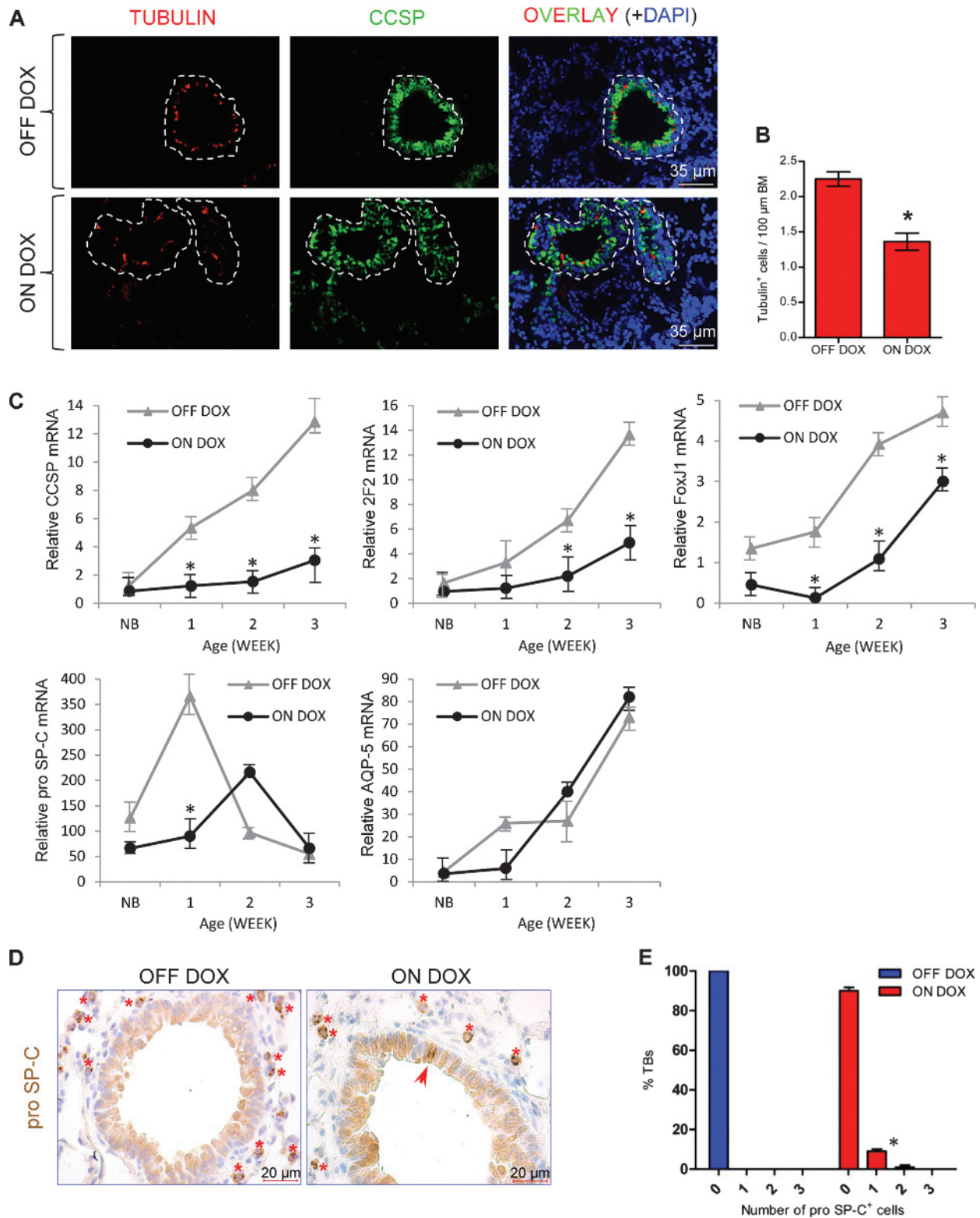
Figure 2. Disruption of E-cadherin in Scgb1a1-expressing cells impairs Clara cell lineage differentiation and induces ectopic expression of pro SpC in conducting airways. (A) Representative dual immunofluorescence staining of lung sections for tubulin (red) and Scgb1a1 (green). Individual bronchioles are encircled by dashed lines. Nuclei were counterstained with DAPI (blue). (B) Morphometric analysis of ciliated cells. Results are presented as means ± SEM for each group. *$P < .05$. BM, basement membrane. (C) Gene expression as a function of age. Total lung RNA from control and induced mice was assayed for expression of Scgb1a1, cytochrome $P450$-2F2, FoxJ1, SpC, and AQP-5 by quantitative RT-PCR, and average ddC$_T$ values are presented ± SEM. NB, new born. (D) Immunohistochemistry shows ectopic expression of the alveolar type II cell marker pro Sftpc (red arrow) in bronchiolar epithelium of an induced mouse. Type II pneumocytes (red asterisks) served as an internal control for pro Sftpc staining (brown). Hematoxylin (blue) was used as a counterstain. (E) The percentage of terminal bronchioles containing zero, one, and two cells with ectopic pro Sftpc expression is shown. At least 220 bronchioles were counted from six DTR mice for each group. Results are presented as means ± SEM for each group. *$P < .05$.
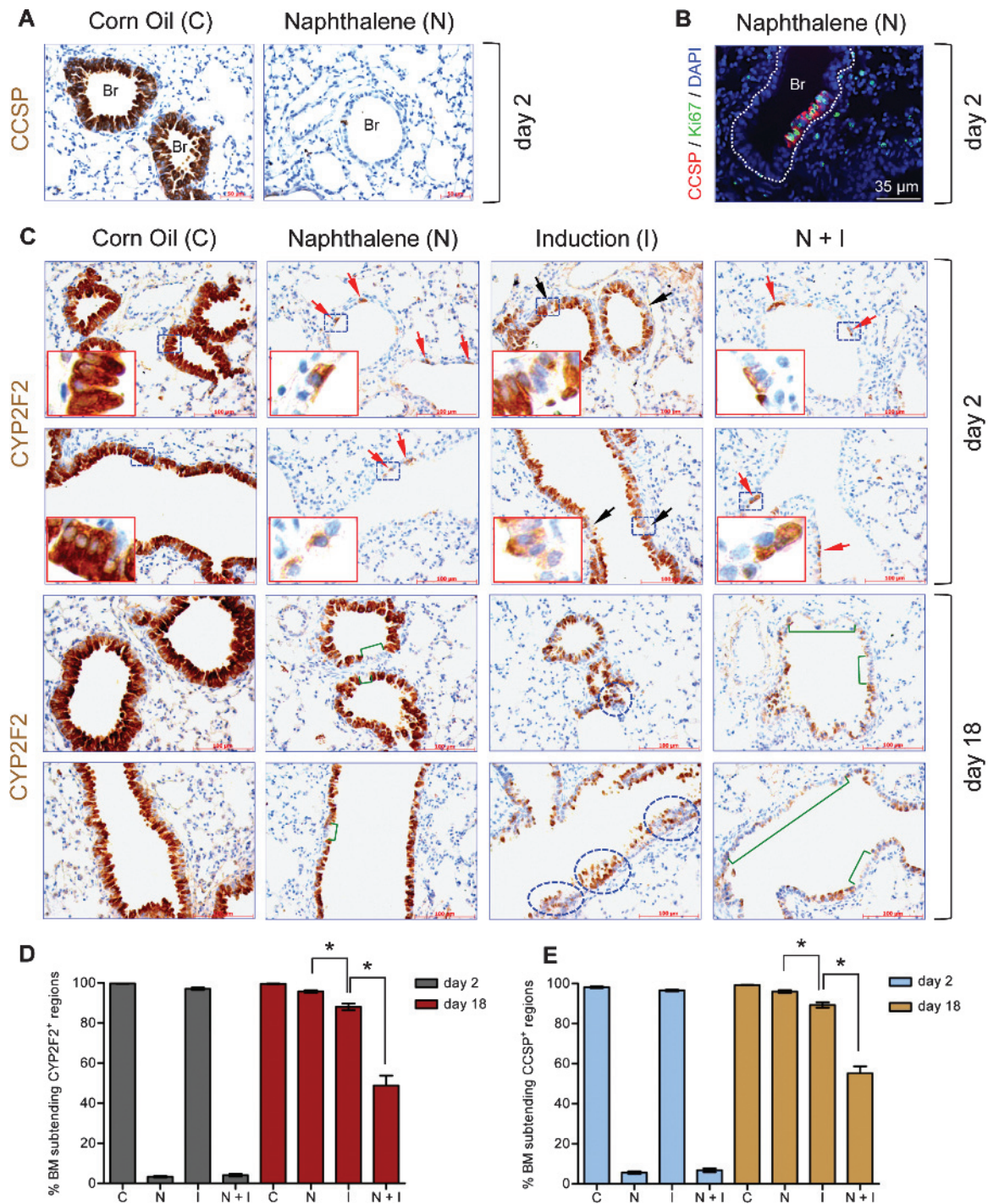
Figure 3. E-cadherin is necessary for the repair of conducting airway epithelium after injury. Five-week-old mice were treated as indicated. Mice were recovered following 2 or 18 days from naphthalene or corn oil exposures. (A) Immunohistochemical staining of lung sections for Scgb1a1. Images are representative of $n = 4$ separate mice per treatment group. Br, bronchiole. (B) Double immunofluorescence staining of a lung section for Scgb1a1 (red) and Ki67 (green) shows actively proliferating naphthalene-resistant Clara cells in bronchiolar epithelium of a medium airway (dotted line) 2 days after naphthalene treatment. Nuclei were counterstained with DAPI (blue). (C) Immunohistochemical staining of lungs sections for CYP2F2. Red arrows indicate naphthalene-resistant Clara cells. Black arrows and green brackets indicate Scgb1a1-negative regions. Insets represent higher magnification of the areas shown in boxed areas. Blue circles indicate increased cellular densities. Hematoxylin (blue) was used as a counterstain. (D and E) Morphometric quantification of the epithelial damage at day 2 and day 18 after naphthalene-mediated injury. The impact of treatment on epithelial repair was determined through analysis of Scgb1a1 (E) or CYP2F2 (D) repopulation. Results are presented as means ± SEM for each group ($n = 4$). *$P < .05$. BM, basement membrane.
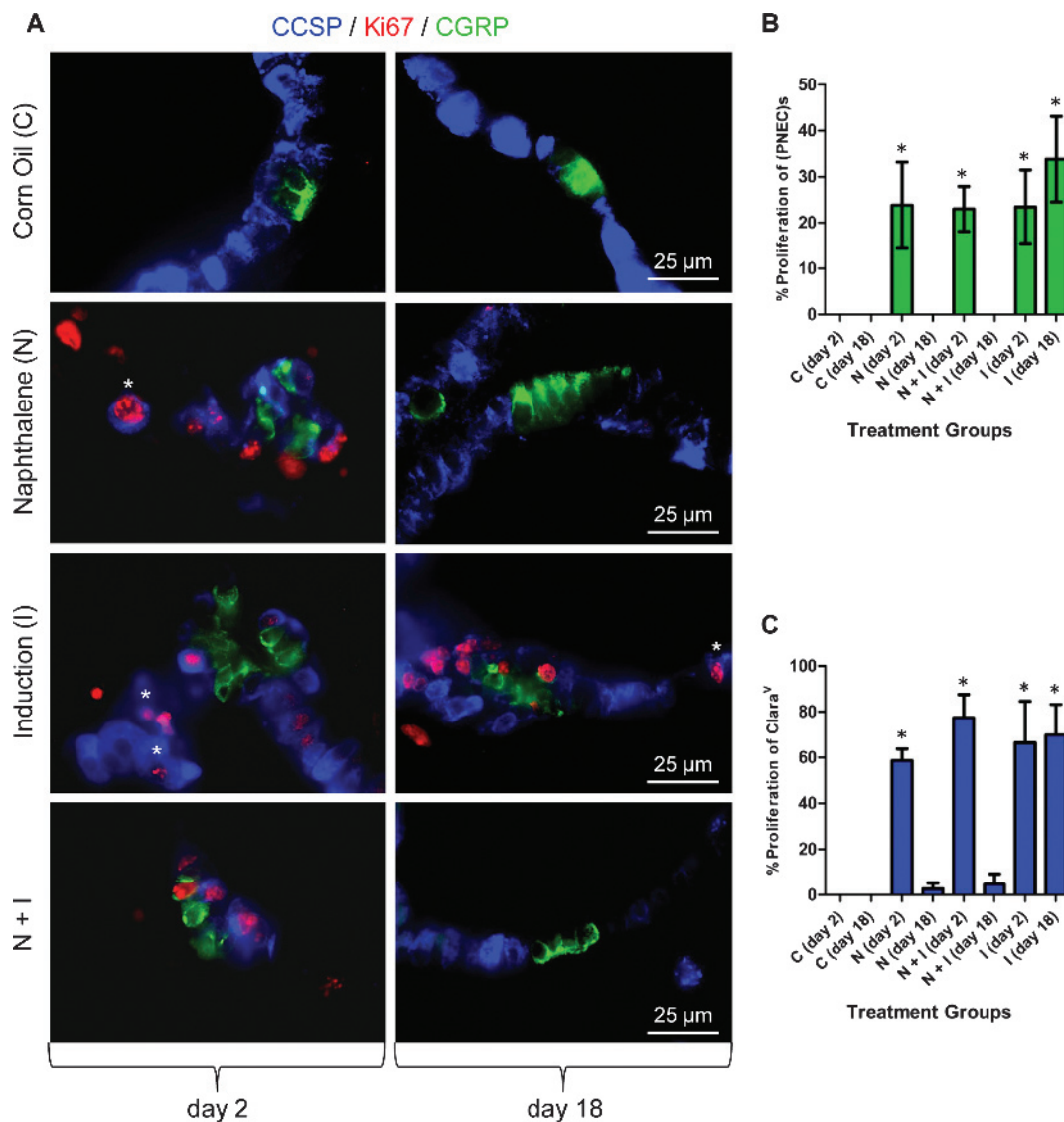
Figure 4. Analysis of cell proliferation within NEB regions under airway repair and steady-state conditions after E-cadherin inactivation. (A) Triple immunofluorescence staining of lung sections for indicated markers. Naphthalene-resistant Clara cells (Clara^V) were identified with their close association with CGRP-expressing neuroendocrine cells in NEBs. Asterisks show proliferating Clara cells that are NEB-independent. Nuclei were counterstained with DAPI (blue). Quantitation of cell proliferation for PNECs (B) and for Clara^V cells (C) for indicated treatment groups. Results are presented as average ± SEM for each group ($n = 4$). *$P < .05$.

patterning. To assess whether the cells ectopically expressing pro Sftpc also expressed Scgb1a1, dual immunofluorescence staining was performed. Cells stained for Sftpc within the conducting airways were also positive for Scgb1a1, indicating that these represented BASC-like progenitor cells (Figures 5A). Despite ectopic localization, the level of BASC-like progenitor cells was indistinguishable between the DOX-treated and untreated groups (Figure 5, B and C), suggesting that E-cadherin controls location rather than the expansion of this cell type. Because activation of canonical Wnt signaling was shown to regulate BASCs during lung epithelial regeneration [33], we sought to determine the activation of β-catenin signaling in conducting airways after DOX induction. Staining of lung sections with an antibody that specifically detects the non-phosphorylated (stabilized) form of β-catenin did not show discernible staining in corn oil–treated control mice (Figure W6A). Consistent with activation of canonical Wnt/β-catenin signaling during lung epithelial regeneration [33], acute naphthalene treatment of DTR

mice elicited nuclear β-catenin localization in naphthalene-resistant Clara cells that was no longer detectable after airway restoration (Figure W6, A and B). As in the case of naphthalene-treated animals, we observed abundant β-catenin nuclear localizations in the majority of the conducting airway cells after 2 days of DOX administration, indicating activation of β-catenin signaling (Figure W6A). Conducting airway epithelial cells with nuclear β-catenin staining were also detected in 18-day DOX-induced DTR mice, albeit at low numbers (Figure W6B). To determine whether the observed nuclear β-catenin localization detected in lung sections from induced DTR mice correlates with activation of the known canonical Wnt target genes, we performed semiquantitative RT-PCR and Western blot analysis. The results of these experiments showed that expression of dn E-cadherin indeed activates this pathway (Figure W6, C and D). Taken together, these data indicate that E-cadherin plays an essential role in the regulation of bronchiolar stem cells in a steady-state adult lung and its disruption affects differentiation

rather than the maintenance of these stem cells after airway injury presumably through activation of canonical Wnt signaling.

Loss of E-cadherin Function in Scgb1a1-expressing Cells Causes Bronchiolar Hyperplasia that Are Rarely Progressing to Lung Cancer

Continued proliferation of Clara^V cells as well as the hypercellularity that we noted in the conducting airways of 18-day induced DTR mice (Figure 3C) suggested that loss of E-cadherin in the epithelium of conducting airways elicits precancerous lesions. We therefore screened a large cohort of DTR mice that were treated with different

DOX schedules for the incidence of hyperplasia. Focal epithelial hyperplasia characterized by a hypercellular epithelium that protruded into bronchial and bronchiolar lumens was observed as early as 2 weeks of DOX treatment (Figure 7A). Such bronchiolar hyperplasia was rarely detected in a very small fraction of the conducting airways of control mice. This might be attributed to known off-target toxicity of *rtTA* or low-level leakiness of the tet system (Figure 7B) [34]. In accordance with the abnormal proliferation of Clara^V and PNE cells (Figure 4, A–C) in induced DTR mice, early focal hyperplastic lesions stained positive for PGP 9.5, a marker for NE cells, and Scgb1a1, indicating that these preneoplastic lesions represent an expansion of these
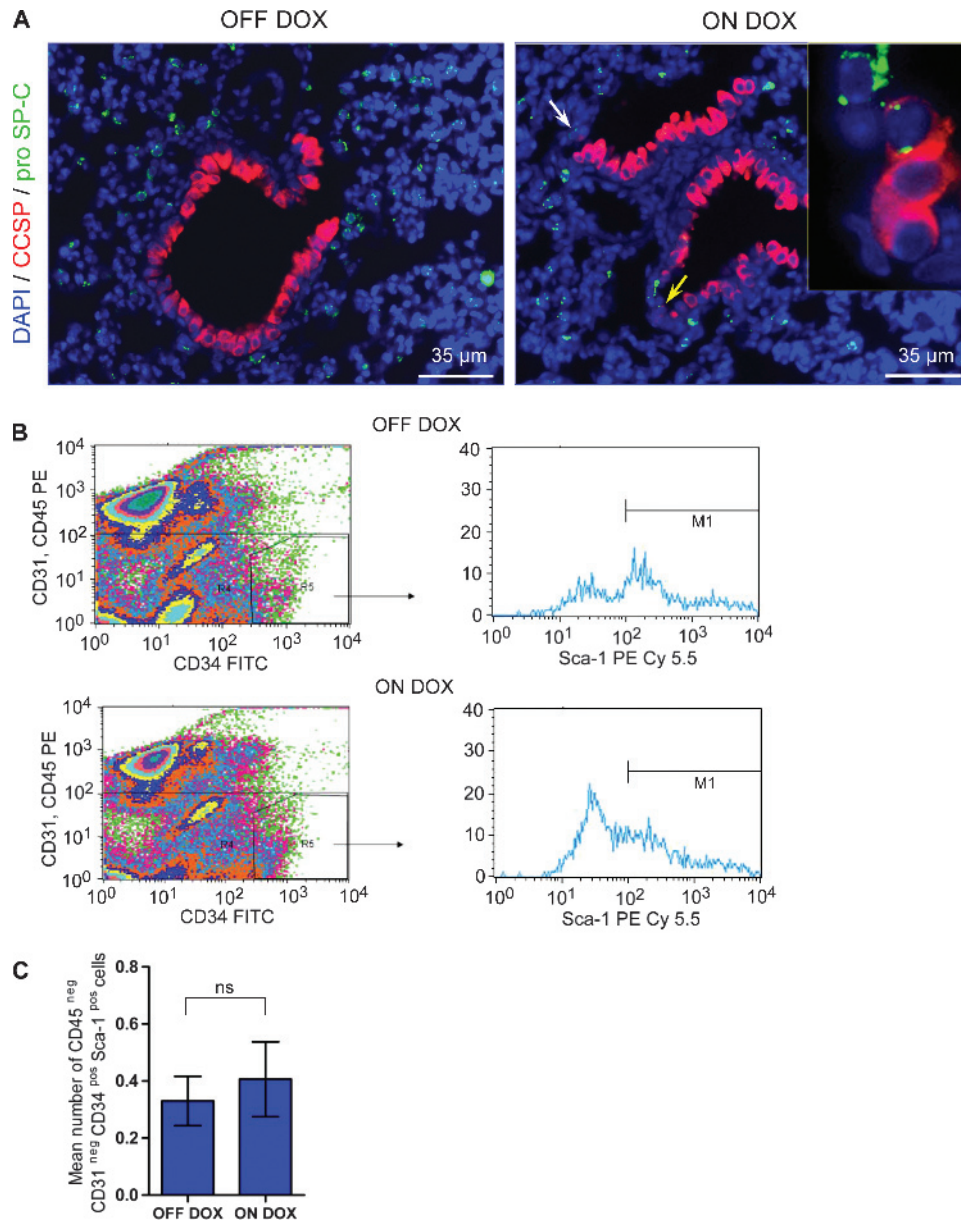
Figure 5. Clara cell–specific loss of E-cadherin in adult lungs leads to ectopic BASC-like progenitor cell localization. (A) Representative double immunofluorescence staining of lung sections for pro Sftpc (green) and Scgb1a1 (red) shows ectopic BASC-like progenitor cell localizations (arrows) in an induced mouse compared to control. Yellow arrow indicates the region shown in the inset. Nuclei were counterstained with DAPI (blue). (B) Gating strategy for FACS sorting. Cells were first gated on the CD31/CD45^{neg} and CD34^{pos} population and then subsequently gated on the Sca1^{pos} population. (C) Quantitation of flow cytometry for BASC-like progenitor cells between the uninduced (OFF DOX) and 1-month DOX-induced (ON DOX) DTR mice ($n = 3$ mice for each group). Results are presented as means ± SEM for each group. ns, statistically not significant.
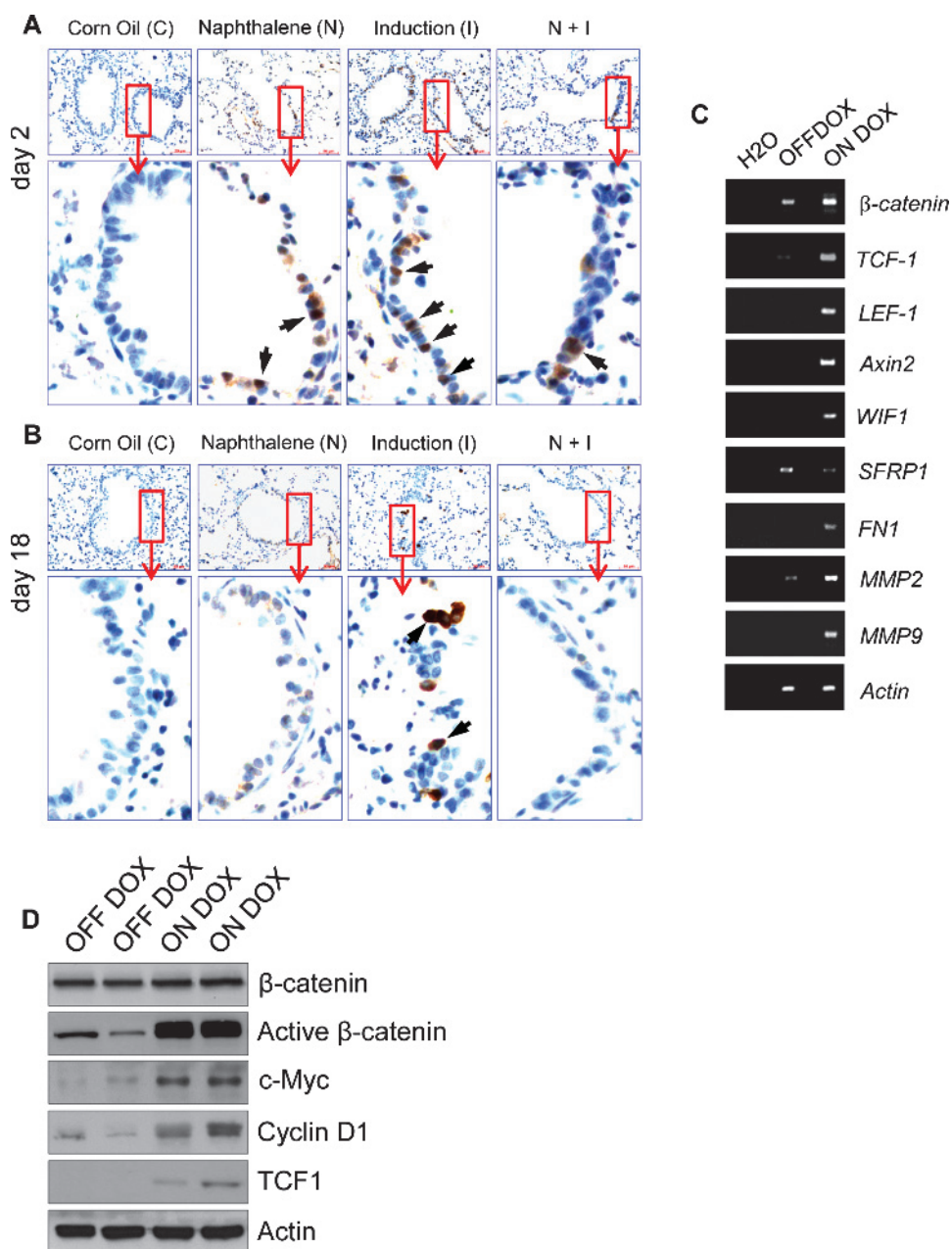
Figure 6. Activation of canonical Wnt signaling upon airway injury or as a consequence of dn E-cadherin expression in conducting airway epithelium. (A and B) Immunohistochemistry of lung sections for β-catenin. Duration and type of treatment as indicated. High-magnification images represent regions shown in insets. Arrows show nuclear staining of β-catenin (brown). Hematoxylin (blue) was used as a counterstain. (C) Semiquantitative RT-PCR analysis of Wnt/β-catenin–regulated genes for control (OFF DOX) and induced (ON DOX) DTR mice. Actin was used as an internal control. (D) Immunoblot analysis of total lung lysates of control and induced DTR mice with the indicated markers.

progenitor cells (Figure 7*C*). Analysis of transgene expression by immunofluorescence staining showed that the majority of the hyperplastic cells lost dn E-cadherin expression at this stage (Figure W3). Prolongation of DOX treatment led to the occurrence of an extensive papillary hyperplasia throughout the conducting airways (Figure 7*D*). Consistent with the loss of Scgb1a1 staining in dn E-cadherin–expressing Clara cells (Figures 1*D* and 3*E*), immunohistochemical analysis showed that the majority of cells in the hyperplastic regions were negative or weakly stained for Scgb1a1 (Figure 7*D*). Similar to dn E-cadherin–expressing conducting airway epithelium, most of the hyperplastic cells showed nuclear β-catenin expression (Figure W4*A*). Despite activation of

canonical Wnt signaling in a certain fraction of hyperplastic cells, there was no Sftpc or Sftpc/Scgb1a1 dual expressions in the hyperplastic lesions (Figure W4*B*). To further identify the nature of the Scgb1a1-negative cells in these hyperplastic regions, we stained them for markers of ciliated and goblet cells, the other cell types that reside in the conducting airways. Consistent with the loss of Clara cell differentiation, there was no expansion of these cells in the preneoplastic lesions (Figure W5, *A* and *B*).

Despite the progressive hyperplasia, multifocal pulmonary tumors of epithelial origin were only observed in 3 of 28 induced DTR mice analyzed between 10 and 18 months of age. Such multifocal lung

tumors were never observed in control DTR or single transgenic mice. As in the case of 2 of 27 control DTR mice, 3 animals from the remaining induced DTR mice developed single pulmonary foci reminiscent of spontaneous lung tumors. Histologic examination of lung sections from multifocal tumor-bearing mice demonstrated solid lung tumors, which were unevenly distributed between the lung lobes (Figure 8*A*). Morphologically, these lung tumors resembled papillary hyperplasias (Figure W6, *A* and *B*). Microscopic examination of histopathology demonstrated that these tumors are malignant invasive adenocarcinomas presenting a predominant papillary columnar growth pattern with some additional micropapillary spots (Figure 8*C*). Staining of lung tumor sections with Ki67 antibody showed that most of the tumor cells were actively proliferating (Figure 8*A*). Both columnar and cuboidal lung tumors stained uniformly for TTF-1 but mostly lacked
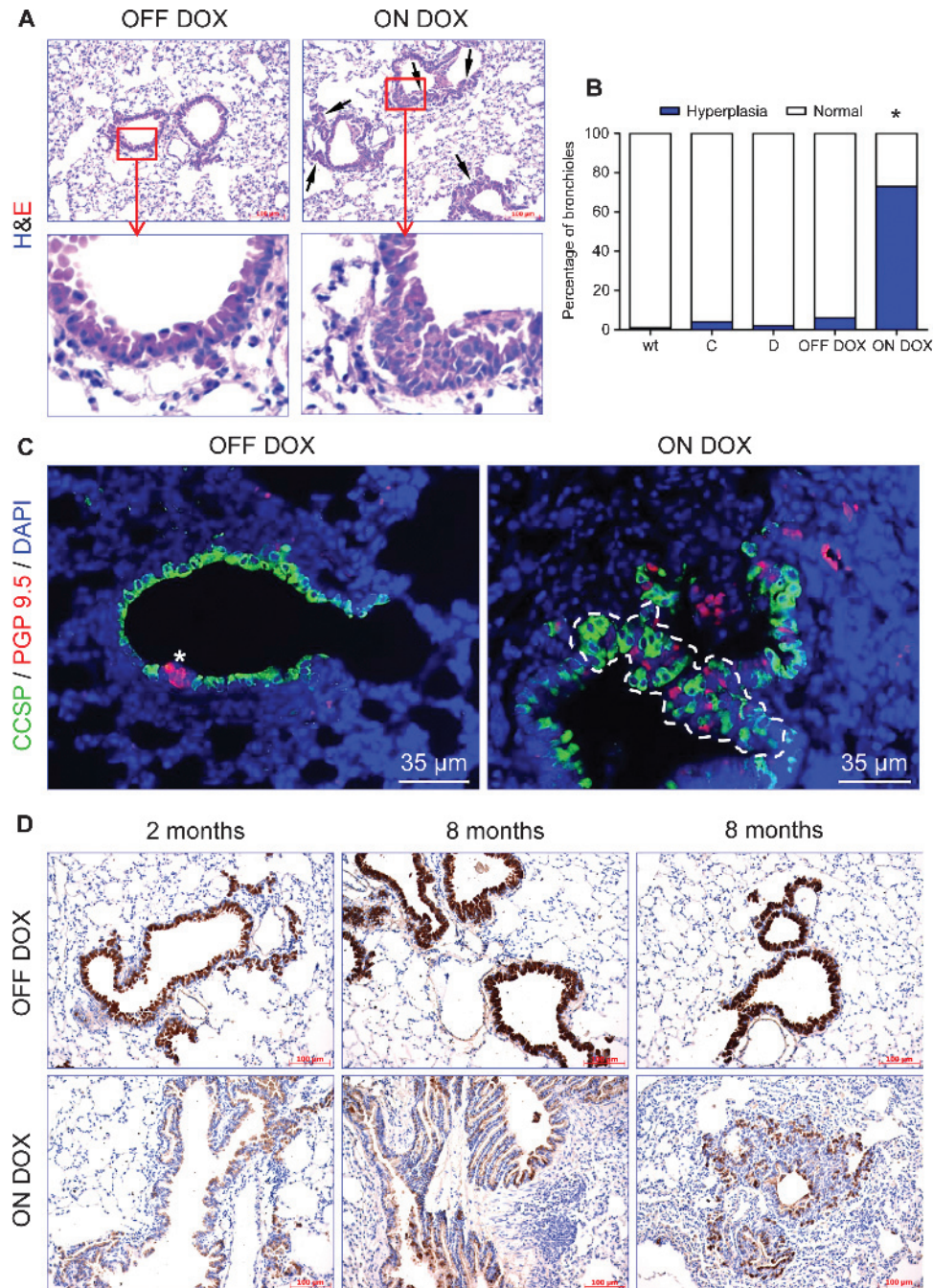
Figure 7. Loss of E-cadherin expression in conducting airway epithelium leads to bronchiolar hyperplasia. (A) Histologic analysis through H&E staining of lungs from control and 2-week DOX-treated DTR mice showing the presence of epithelial hyperplasia (arrow). (B) Quantitation of bronchiolar hyperplasia between the mice groups: wt, wild type ($n = 13$), (C) *Scgb1a1-rtTA* ($n = 27$), (D) *Tet-O* dn E-cadherin ($n = 23$), DTR OFF DOX ($n = 39$), DTR ON DOX ($n = 40$); *$P < .05$. (C) Double immunofluorescence staining of the same lung sections from A for indicated markers. Asterisk shows a PGP 9.5-positive NEB region. Marked region shows an expansion of an NEB region consisting of PGP 9.5-and Scgb1a1-positive cells after induction. Nuclei were counterstained with DAPI (blue). (D) Immunohistochemical staining of lung sections for Scgb1a1. Images are representative of $n = 6$ mice in each group. Hematoxylin (blue) was used as a counterstain.
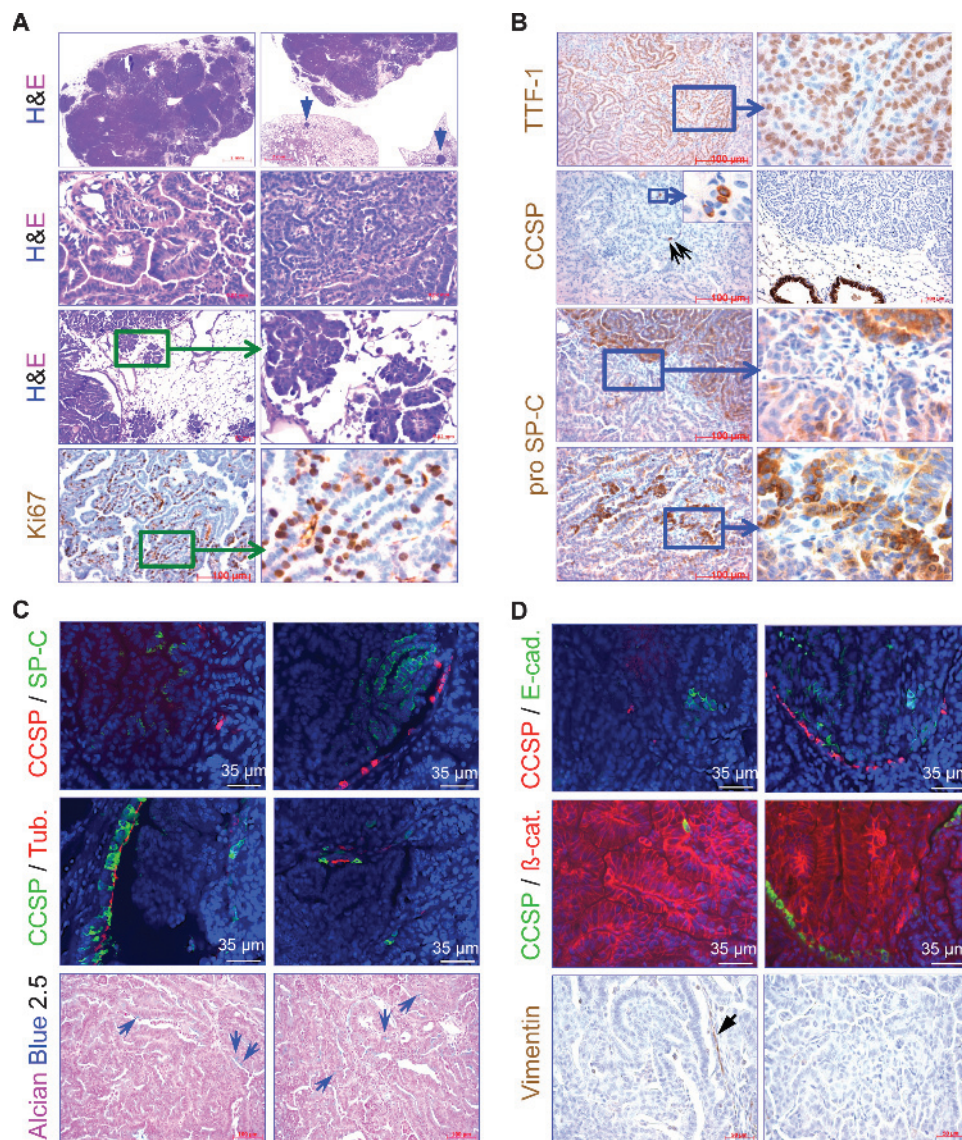
Figure 8. Analysis of incidence and histopathology of pulmonary tumors from induced transgenic mice. (A) Lung sections from tumor-bearing mice were either H&E stained or immunostained for Ki67 (brown). Arrows indicate tumor foci. (B) Immunohistochemistry of tumor-bearing lung sections for lung differentiation markers as indicated. Arrows show rare Scgb1a1-positive tumor cells that were never detected in spontaneous lung tumor but in their surrounding bronchioles. (C and D) Staining of lung tumor sections with the indicated markers. Arrows in C show Alcian Blue–positive vessel and those in D show vimentin-positive vessel. Two representative pictures were shown for each staining.

staining for Scgb1a1, indicating that tumors were not highly differentiated (Figure 8B). Similar to the induced hyperplastic lesions, only a minority of the tumor cells expressed the transgene (Figure W7A). Neither Scgb1a1 (Figure 8B) nor the transgene expression (Figure W7A) was detected in spontaneous lung tumors. In treated DTR mice, the two subtypes of multifocal lung tumors not only differed in their morphology but also with respect to their pro Sftpc expression. Compared to the uniform staining pattern of cuboidal tumors, only a minor fraction of columnar tumors contained pro Sftpc–positive cells with cuboidal morphology, suggesting that cuboidal tumors arise from columnar tumors by a dedifferentiation mechanism (Figure 8B). None of the pro Sftpc–expressing tumor cells stained positive for Scgb1a1, indicating that these do not represent BASC-like progenitor cells (Figure 8C). As in the case of the bronchiolar hyperplasia, tumor cells both from cuboidal and columnar tumors did not contain ciliated or goblet cells

except the bronchiolar epithelium that is often embedded in the tumor (Figure 8C). Although the majority of tumor cells lost the transgene expression (Figure W7A), the great majority of the tumor cells lacked E-cadherin but not β-catenin expression (Figure 8D). Interestingly, despite the invasive features, tumor cells did not show detectable vimentin expression or other epithelial-mesenchymal transition (EMT) markers (Figure W8) after E-cadherin loss, indicating that EMT program was not activated in tumor cells (Figure 8D). Consistent with the lack of EMT, we did not detect disseminating tumor cells in other organs (data not shown).

Low incidence of lung tumors as well as their maintenance in the absence of the transgene expression supports the existence of additional genetic alterations. We therefore screened DNA samples from individual lung tumors for the incidence of *K-ras* mutation, the most frequent type of mutation found in human non–small cell lung cancer

Table 1. Lung Tumors from Induced Mice Carry *K-ras* Mutation at Position 12.

	Exon 1	Exon 2
Tumor sample 1	GGT > CGT	wt
Non-tumor sample 1	wt	wt
Bronchiolar hyperplasia 1	wt	wt
Tumor sample 2	GGT > CGT	wt
Non-tumor sample 2	wt	wt
Bronchiolar hyperplasia 2	wt	wt
Tumor sample 3	GGT > CGT	wt
Non-tumor sample 3	wt	wt
Bronchiolar hyperplasia 3	wt	wt

(NSCLC). Sequencing of exons 1 and 2 of the *K-ras* gene demonstrated an amino acid substitution at position 12, from glycine to arginine (GGT→CGT, K-ras^{G12R}). This mutation confers constitutive activity of the ras-guanosine triphosphatase (GTPase). The G12R mutation was undetectable in non-neoplastic regions of the lung and the bronchiolar hyperplasia (Table 1). Consistent with *K-ras*^{G12R} mutation, lung tumors stained positive for the active form of Akt (pAkt) and ERK (pERK), two downstream effectors of *K-ras* signaling (Figure W7, *B* and *C*). These results demonstrate that expression of a dn E-cadherin mutant in the conducting airways induces the onset of preneoplastic lung lesions that may predispose mice to lung cancer after cooperating genetic alteration.

Discussion

In the present study, we have investigated the role of E-cadherin in non-ciliated Clara cells of the bronchiolar airways as these cells were shown to represent progenitor/stem cells of the conducting airways and have been discussed as the cell of origin of human NSCLC [35]. Our results demonstrate that E-cadherin is necessary for maintenance of Clara cell differentiation. Inactivation of E-cadherin impaired the repair of conducting airway epithelium after injury in part by altering the differentiation potential of bronchiolar stem cells. Loss of E-cadherin expression in steady-state adult lung caused papillary epithelial cell hyperplasia in the bronchial and bronchiolar lumens, providing evidence that E-cadherin is required for the normal regulation of epithelial cell proliferation in the lung. Despite progressive hyperplasia, formation of lung tumors was a rare event and required a cooperating genetic insult.

The respiratory epithelium of conducting airways plays a critical role in pulmonary homeostasis, maintaining barrier function and sterility. Previous studies have established an important role of canonical Wnt signaling in lung development, lung cell differentiation, and lung stem cell homeostasis. Three independent studies have shown that stabilization of β-catenin in Clara cells causes loss of Scgb1a1 staining and blocks Clara cell differentiation to the ciliated cell lineage [36–38]. In line with nuclear β-catenin accumulation in conducting airway epithelial cells, it is likely that the perturbation of Clara cell differentiation upon expression of dn E-cadherin in Scgb1a1-expressing cells is mediated by activation of canonical Wnt signaling. Activation of Wnt/β-catenin signaling following reduction in E-cadherin levels has previously been described in several model systems [39–41]. In addition to perturbation of Clara cell differentiation, we detected pro Sftpc expression in the bronchioles of the E-cadherin–deficient mice. Interestingly, ectopic pro Sftpc expression was also reported in a study in which a non-degradable β-catenin was expressed in mouse Clara cells [37] further supporting our observation of β-catenin activation in the DTR system. Further characterization revealed that these cells have some

molecular similarities to BASCs. BASCs are regional stem cell population in the distal lung and are normally located at BADJ. Transient proliferation of BASCs at BADJ regions was reported to be a consequence of naphthalene exposure [17]. Increased number of BASCs was also reported upon forced expression of stabilized β-catenin in Clara cells [33]. In the present work, despite activation of Wnt signaling and appearance of BASC-like progenitor cells at ectopic sites, the total level of BASC-like progenitor cells did not alter significantly between the control and induced DTR mice. The failure in detecting increased BASC-like progenitor cell numbers in induced DTR mice may result from a low abundance of ectopic pro Sftpc expression in conducting airways. Alternatively, there might be molecular differences between ectopic BASC-like progenitor cells and BASCs that normally reside at the BADJ in terms of the markers (CD31, CD45, CD34, Sca1) that we used for sorting. If this would be the case, the ectopic pro Sftpc expression may simply represent an altered differentiation rather than true stem cell behavior. We do not yet understand the physiological importance of these rare cells.

Genetic inactivation of E-cadherin in Scgb1a1-expressing epithelial cells not only caused appearance of BASC-like progenitor cells at ectopic sites but also resulted in generation of other immature cell types such as NEB-associated Clara cells (Clara^V). The lack of Clara and ciliated cells in conducting airways of induced DTR mice suggests that the delicate balance between these progenitor/stem and differentiated cells is impaired. The normal proliferation of Clara^V cells during airway regeneration suggests that the airway repair defects observed in DOX-treated (dn E-cadherin–expressing) DTR mice resulted from failure of these stem cells to generate differentiated epithelial cell types rather than their maintenance.

In contrast to what we observed after lung injury, postnatal loss of E-cadherin function in conducting airways of the steady-state lung resulted in a hyperproliferative response of Clara^V cells that led to bronchiolar hyperplasia. The presence of incessantly dividing Clara^V cells in these early hyperplastic foci suggested a bronchiolar stem cell origin for these precancerous lesions. Under normal physiological conditions, upon bronchiolar damage, i.e., naphthalene exposure, NEB-associated Clara^V cells start to proliferate to renew conducting airway epithelium. It is conceivable that loss of bronchiolar integrity upon E-cadherin inactivation similarly evokes a repair response leading to the proliferation of Clara^V cells. In contrast to a normal repair condition where NEB-associated Clara^V cells become quiescent after renewal, unremitting proliferation of these progenitors in E-cadherin–deficient conducting airway epithelium suggests that these bronchiolar stem cells account for the observed bronchiolar hyperplasia.

Down-regulation of E-cadherin is a hallmark of most malignant human tumors with epithelial origin including lung cancer. Frequent loss of E-cadherin has been observed in human intrabronchial lesions during carcinogenesis of the bronchial epithelium [42]. In the current study, although the majority of the mice developed bronchiolar hyperplasia to different degrees, the incidence of pulmonary tumors was low. Formation of rare pulmonary tumors was also reported in transgenic mice in which an activated form of β-catenin [Catnb$^{\Delta(ex3)}$] was expressed in Clara cells [37]. Lack of progression from hyperplasia to overt lung tumors in the majority of the animals in the present model might result from loss of Scgb1a1 expression. Earlier studies have shown that down-regulation of Scgb1a1 is an early event during pulmonary carcinogenesis and only a small percentage of tumor cells expresses Scgb1a1 [43]. Despite a selective advantage of Scgb1a1 down-regulation during lung cancer progression, this loss of Scgb1a1 expression in the observed

bronchiolar hyperplasia may elicit the shutdown of transgene expression, which can explain the block in progression to overt tumor formation. Alternatively, in line with a multistep tumorigenesis model, bronchiolar hyperplasia might require an additional epigenetic or genetic alteration for further progression. In fact, detection of *K-ras* mutations (G12R) in all lung tumors but not in bronchiolar hyperplasias of the DOX-treated (dn E-cadherin–expressing) mice supports this hypothesis. Moreover, absence of multiple pulmonary tumors in control animals suggests cooperation between the loss of functional E-cadherin and oncogenic *K-ras* in the development of lung cancer.

The cellular heterogeneity within a tumor hampers the identification of a cell of origin, particularly if a characteristic cell marker such as Scgb1a1 is downregulated upon neoplastic conversion and the cell of interest is phenotypically plastic. Pro Sftpc is often expressed in lung tumors in mice. Whether this is because tumors arise from alveolar type II cells or because cancer cells gain pro Sftpc expression is still unclear. Expression of pro Sftpc in the DOX-treated tumors in which Scgb1a1 was down-modulated brings an explanation to the lung tumor animal models in which the candidate oncogene has been expressed under the control of the *Scgb1a1* promoter and pulmonary tumors with type II cell features were formed. Our recent publication regarding the formation of bronchiolar hyperplasia that are negative for Scgb1a1 and positive for pro Sftpc upon conditional expression of oncogenic C-RAF in Clara cells supports this hypothesis [44]. In animal model studies, three cell types of pulmonary lineage, namely, type II pneumocytes, Clara cells, and BASCs, have so far been identified as cells of origin of lung adenocarcinomas [35]. To our knowledge, our results provide the first *in vivo* data in addition to these cells; NEB-associated naphthalene-resistant Clara cells (Clara^V) play an important role in the formation of precancerous lesions, increasing the susceptibility to lung cancer. When compared to lung tumors, lack of *K-ras* G12R mutation in precancerous lesions of DOX-treated mice supports the notion that expansion of stem/progenitor cells alone is not sufficient for tumorigenesis but requires at least one further genetic or epigenetic event [45].

Our data demonstrate that E-cadherin is necessary for the homeostasis of the epithelial cells lining the conducting airways. Overexpression of dn E-cadherin in Scgb1a1-expressing cells resulted in dramatic reduction in the abundance of two derivatives of bronchiolar stem cells, the differentiated Clara cell and the terminally differentiated ciliated cell. The lack of differentiated cell types was accompanied by a corresponding increase in the number of immature epithelial cells that were identified either as BASC-like progenitor cells or Clara^V cells. Thus, disruption of cell adhesion between Clara cells of the steady-state lung potentially generated a population of bronchiolar stem cells that failed to generate differentiated epithelial cell types. This might be the potential cause of defective airway regeneration after injury. Uncontrolled expansion of Clara^V cells following functional loss of E-cadherin in mature Clara cells resulted in bronchiolar hyperplasia that predisposed the lungs to tumor formation.

Acknowledgments

References

[1] Maeda Y, Dave V, and Whitsett JA (2007). Transcriptional control of lung morphogenesis. *Physiol Rev* **87**, 219–244.

[2] Blenkinsopp WK (1967). Proliferation of respiratory tract epithelium in the rat. *Exp Cell Res* **46**, 144–154.

[3] Evans MJ, Cabral LC, Stephens RJ, and Freeman G (1974). Acute kinetic response and renewal of the alveolar epithelium following injury by nitrogen dioxide. *Chest* **65**(suppl), 62S–65S.

[4] Evans MJ, Cabral LJ, Stephens RJ, and Freeman G (1975). Transformation of alveolar type 2 cells to type 1 cells following exposure to NO$_2$. *Exp Mol Pathol* **22**, 142–150.

[5] Hong KU, Reynolds SD, Watkins S, Fuchs E, and Stripp BR (2004). Basal cells are a multipotent progenitor capable of renewing the bronchial epithelium. *Am J Pathol* **164**, 577–588.

[6] Schoch KG, Lori A, Burns KA, Eldred T, Olsen JC, and Randell SH (2004). A subset of mouse tracheal epithelial basal cells generates large colonies *in vitro*. *Am J Physiol Lung Cell Mol Physiol* **286**, L631–L642.

[7] Giangreco A, Reynolds SD, and Stripp BR (2002). Terminal bronchioles harbor a unique airway stem cell population that localizes to the bronchoalveolar duct junction. *Am J Pathol* **161**, 173–182.

[8] Rawlins EL and Hogan BL (2006). Epithelial stem cells of the lung: privileged few or opportunities for many? *Development* **133**, 2455–2465.

[9] Warburton D, Perin L, Defilippo R, Bellusci S, Shi W, and Driscoll B (2008). Stem/progenitor cells in lung development, injury repair, and regeneration. *Proc Am Thorac Soc* **5**, 703–706.

[10] Evans MJ, Johnson LV, Stephens RJ, and Freeman G (1976). Renewal of the terminal bronchiolar epithelium in the rat following exposure to NO$_2$ or O$_3$. *Lab Invest* **35**, 246–257.

[11] Evans MJ, Cabral-Anderson LJ, and Freeman G (1978). Role of the Clara cell in renewal of the bronchiolar epithelium. *Lab Invest* **38**, 648–653.

[12] Reynolds SD, Hong KU, Giangreco A, Mango GW, Guron C, Morimoto Y, and Stripp BR (2000). Conditional Clara cell ablation reveals a self-renewing progenitor function of pulmonary neuroendocrine cells. *Am J Physiol Lung Cell Mol Physiol* **278**, L1256–L1263.

[13] Rawlins EL, Okubo T, Xue Y, Brass DM, Auten RL, Hasegawa H, Wang F, and Hogan BL (2009). The role of Scgb1a1$^+$ Clara cells in the long-term maintenance and repair of lung airway, but not alveolar, epithelium. *Cell Stem Cell* **4**, 525–534.

[14] Reynolds SD and Malkinson AM (2010). Clara cell: progenitor for the bronchiolar epithelium. *Int J Biochem Cell Biol* **42**, 1–4.

[15] Hong KU, Reynolds SD, Giangreco A, Hurley CM, and Stripp BR (2001). Clara cell secretory protein-expressing cells of the airway neuroepithelial body microenvironment include a label-retaining subset and are critical for epithelial renewal after progenitor cell depletion. *Am J Respir Cell Mol Biol* **24**, 671–681.

[16] Reynolds SD, Giangreco A, Power JH, and Stripp BR (2000). Neuroepithelial bodies of pulmonary airways serve as a reservoir of progenitor cells capable of epithelial regeneration. *Am J Pathol* **156**, 269–278.

[17] Kim CF, Jackson EL, Woolfenden AE, Lawrence S, Babar I, Vogel S, Crowley D, Bronson RT, and Jacks T (2005). Identification of bronchioalveolar stem cells in normal lung and lung cancer. *Cell* **121**, 823–835.

[18] Kemler R, Babinet C, Eisen H, and Jacob F (1977). Surface antigen in early differentiation. *Proc Natl Acad Sci USA* **74**, 4449–4452.

[19] Larue L, Ohsugi M, Hirchenhain J, and Kemler R (1994). E-cadherin null mutant embryos fail to form a trophectoderm epithelium. *Proc Natl Acad Sci USA* **91**, 8263–8267.

[20] Riethmacher D, Brinkmann V, and Birchmeier C (1995). A targeted mutation in the mouse E-cadherin gene results in defective preimplantation development. *Proc Natl Acad Sci USA* **92**, 855–859.

[21] Young P, Boussadia O, Halfter H, Grose R, Berger P, Leone DP, Robenek H, Charnay P, Kemler R, and Suter U (2003). E-cadherin controls adherens junctions in the epidermis and the renewal of hair follicles. *EMBO J* **22**, 5723–5733.

[22] Tinkle CL, Lechler T, Pasolli HA, and Fuchs E (2004). Conditional targeting of E-cadherin in skin: insights into hyperproliferative and degenerative responses. *Proc Natl Acad Sci USA* **101**, 552–557.

[23] Boussadia O, Kutsch S, Hierholzer A, Delmas V, and Kemler R (2002). E-cadherin is a survival factor for the lactating mouse mammary gland. *Mech Dev* **115**, 53–62.

[24] Hirai Y, Nose A, Kobayashi S, and Takeichi M (1989). Expression and role of E- and P-cadherin adhesion molecules in embryonic histogenesis. I. Lung epithelial morphogenesis. *Development* **105**, 263–270.

[25] Ceteci F, Ceteci S, Karreman C, Kramer BW, Asan E, Gotz R, and Rapp UR (2007). Disruption of tumor cell adhesion promotes angiogenic switch and progression to micrometastasis in RAF-driven murine lung cancer. *Cancer Cell* **12**, 145–159.

[26] Cavallaro U and Christofori G (2004). Cell adhesion and signalling by cadherins and Ig-CAMs in cancer. *Nat Rev Cancer* **4**, 118–132.

[27] Onder TT, Gupta PB, Mani SA, Yang J, Lander ES, and Weinberg RA (2008). Loss of E-cadherin promotes metastasis via multiple downstream transcriptional pathways. *Cancer Res* **68**, 3645–3654.

[28] Dahl U, Sjodin A, and Semb H (1996). Cadherins regulate aggregation of pancreatic β-cells *in vivo*. *Development* **122**, 2895–2902.

[29] Liu C, Glasser SW, Wan H, and Whitsett JA (2002). GATA-6 and thyroid transcription factor-1 directly interact and regulate surfactant protein-C gene expression. *J Biol Chem* **277**, 4519–4525.

[30] Van Winkle LS, Gunderson AD, Shimizu JA, Baker GL, and Brown CD (2002). Gender differences in naphthalene metabolism and naphthalene-induced acute lung injury. *Am J Physiol Lung Cell Mol Physiol* **282**, L1122–L1134.

[31] Wu CA, Peluso JJ, Shanley JD, Puddington L, and Thrall RS (2008). Murine cytomegalovirus influences Foxj1 expression, ciliogenesis, and mucus plugging in mice with allergic airway disease. *Am J Pathol* **172**, 714–724.

[32] Stripp BR, Maxson K, Mera R, and Singh G (1995). Plasticity of airway cell proliferation and gene expression after acute naphthalene injury. *Am J Physiol* **269**, L791–L799.

[33] Zhang Y, Goss AM, Cohen ED, Kadzik R, Lepore JJ, Muthukumaraswamy K, Yang J, DeMayo FJ, Whitsett JA, Parmacek MS, et al. (2008). A Gata6-Wnt pathway required for epithelial stem cell development and airway regeneration. *Nat Genet* **40**, 862–870.

[34] Perl AK, Zhang L, and Whitsett JA (2009). Conditional expression of genes in the respiratory epithelium in transgenic mice: cautionary notes and toward building a better mouse trap. *Am J Respir Cell Mol Biol* **40**, 1–3.

[35] Meuwissen R and Berns A (2005). Mouse models for human lung cancer. *Genes Dev* **19**, 643–664.

[36] Reynolds SD, Zemke AC, Giangreco A, Brockway BL, Teisanu RM, Drake JA, Mariani T, Di PY, Taketo MM, and Stripp BR (2008). Conditional stabilization of β-catenin expands the pool of lung stem cells. *Stem Cells* **26**, 1337–1346.

[37] Mucenski ML, Nation JM, Thitoff AR, Besnard V, Xu Y, Wert SE, Harada N, Taketo MM, Stahlman MT, and Whitsett JA (2005). β-Catenin regulates differentiation of respiratory epithelial cells *in vivo*. *Am J Physiol Lung Cell Mol Physiol* **289**, L971–L979.

[38] Li C, Li A, Li M, Xing Y, Chen H, Hu L, Tiozzo C, Anderson S, Taketo MM, and Minoo P (2009). Stabilized β-catenin in lung epithelial cells changes cell fate and leads to tracheal and bronchial polyposis. *Dev Biol* **334**, 97–108.

[39] Heuberger J and Birchmeier W (2010). Interplay of cadherin-mediated cell adhesion and canonical Wnt signaling. *Cold Spring Harb Perspect Biol* **2**, a002915.

[40] Ma L, Young J, Prabhala H, Pan E, Mestdagh P, Muth D, Teruya-Feldstein J, Reinhardt F, Onder TT, Valastyan S, et al. (2010). miR-9, a MYC/MYCN-activated microRNA, regulates E-cadherin and cancer metastasis. *Nat Cell Biol* **12**, 247–256.

[41] Khew-Goodall Y and Goodall GJ (2010). Myc-modulated miR-9 makes more metastases. *Nat Cell Biol* **12**, 209–211.

[42] Kato Y, Hirano T, Yoshida K, Yashima K, Akimoto S, Tsuji K, Ohira T, Tsuboi M, Ikeda N, Ebihara Y, et al. (2005). Frequent loss of E-cadherin and/or catenins in intrabronchial lesions during carcinogenesis of the bronchial epithelium. *Lung Cancer* **48**, 323–330.

[43] Linnoila RI, Szabo E, DeMayo F, Witschi H, Sabourin C, and Malkinson A (2000). The role of CC10 in pulmonary carcinogenesis: from a marker to tumor suppression. *Ann N Y Acad Sci* **923**, 249–267.

[44] Ceteci F, Xu J, Ceteci S, Zanucco E, Thakur C, and Rapp UR (2011). Conditional expression of oncogenic C-RAF in mouse pulmonary epithelial cells reveals differential tumorigenesis and induction of autophagy leading to tumor regression. *Neoplasia* **13**, 1005–1018.

[45] Peacock CD and Watkins DN (2008). Cancer stem cells and the ontogeny of lung cancer. *J Clin Oncol* **26**, 2883–2889.

Supplementary Materials and Methods

Mouse Strains

Mice were housed under barrier conditions in air-filtered, temperature-controlled units with a 12-hour light/dark cycle with free access to food and water *ad libitum*. *CCSP rtTA* and *Tet-O dn E-cadherin* mice were previously generated and genotyped as described. The dominant negative E-cadherin mutant is a truncated form of E-cadherin lacking most of the extracellular domain inserted with a human c-Myc epitope but still binds β-catenin [1]. *CCSP rtTA* mice were maintained on FVB/n background. *Tet-O dn E-cadherin* transgenic mice were maintained on C57Bl/6 background. Compound mice were induced with DOX (Sigma) containing food (500 mg/kg body weight; Ssniff, Soest, Germany) for different periods and analyzed for the phenotypic accuracy of lung pathology. All animal experiments were performed according to the regulations of the Bavarian State authorities.

RNA Isolation and RT-PCR Analysis

Total RNA was isolated from whole lungs of mice using TRIzol (Invitrogen, Carlsbad, CA) reagent. Samples were treated with RNase-free DNAse I before the preparation of c-DNA using random hexamer primers provided by the First-Strand c-DNA Synthesis Kit (Fermentas, St Leon-Rot, Germany). Control reactions were run using Taq polymerase without reverse transcriptase. Real-time RT-PCR was performed using the DyNAmo HS SYBR Green qPCR Kit (Thermo Fisher Scientific, Erlangen, Germany) in a Roto-Gene 2000 Detection System (Qiagen, Hilden, Germany) with previously described primers [2–4]. Values were calculated by the $\Delta\Delta C_T$ method. RNA of hypoxanthine-guanine phosphoribosyltransferase (HPRT) was used as standard control. Transcriptional activation of the Wnt target genes was determined by semiquantitative RT-PCR using total lung RNA. The PCR products were visualized by electrophoresis in 2% agarose gels. Primer sequences are available on request.

Immunoblot Analysis

Left lung lobes of mice were homogenized shortly using an Ultra-Turrax homogenizer in a cold environment. The homogenates were centrifuged at 11,000 rpm for 10 minutes. After centrifugation, supernatants from samples were analyzed for protein concentration by using the NanoDrop ND-1000 (Thermo Fisher Scientific). The remaining extracts were mixed with 4× Laemmli loading buffer heated to 95°C for 5 minutes and either stored at –20°C or resolved by sodium dodecyl sulfate–polyacrylamide gel electrophoresis and transferred to nitrocellulose membranes. After 1-hour blocking with 5% non-fat dry milk in NET-gelatin (50 mM Tris/HCl (pH 7.4), 5 mM EDTA, 0.05% Triton X-100, 150 mM NaCl, 0.25% gelatin], blots were incubated overnight at 4°C with primary antibodies subsequently washed three times with NET-gelatin and incubated for 1 hour at room temperature with peroxidase-coupled secondary antibodies (GE Healthcare, Freiburg, Germany). After three washes with NET-gelatin, blots were developed using ECL kit (Thermo Fisher Scientific). Immunoblot analysis was performed using the following antibodies: myc tag (9E10, 1:100; Santa Cruz Biotechnology, Offenbach, Germany), actin (I-19, 1:3000; Santa Cruz Biotechnology), E-cadherin (clone ECCD2, 1:250; Zymed Laboratories, Darmstadt, Germany), vimentin (clone D21H3, 1:500; Cell Signaling Technology, Frankfurt, Germany), Slug (clone C19G7, 1:500), N-cadherin (clone 3B9, 1:1000; Invitrogen), c-Myc (clone D84C12, 1:250), cyclin D1 (clone H-295, 1:500; Santa Cruz Biotechnology), TCF1 (clone C63D9, 1:1000; Cell Signaling Technology), β-catenin (clone D10A8, 1:1000), and active β-catenin (clone D13A1, 1:500; Cell Signaling Technology).

Histopathology and Immunostainings

Mouse lungs were dissected and fixed with 4% paraformaldehyde in phosphate-buffered saline (PBS) overnight at 4°C. The tissue samples were rinsed in PBS, dehydrated, and then embedded in paraffin blocks. Six-micrometer tissue sections were deparaffinized, rehydrated in graded series of alcohol, and hematoxylin and eosin (H&E) stained using standard procedures. For immunohistochemistry, sections were deparaffinized and rehydrated. For antigen retrieval, sections were incubated in 10 mM citrate buffer for 10 and 20 minutes using microwave irradiation. Endogenous peroxidase activity was quenched with methanol or PBS containing 1% and 3% H_2O_2. Non-specific binding was blocked with 5% of serum for 1 hour. After blocking, sections were incubated with primary antibodies overnight at 4°C. Immunohistochemistry and immunofluorescent staining was performed using the following antibodies at the indicated dilutions: CYP2F2 (sc-67283, 1:200; Santa Cruz Biotechnology), CCSP (sc-9772, 1:2500; Santa Cruz Biotechnology), Ki67 (MM1, 1:50; Vector Laboratories, Lörrach, Germany), pro SpC (gift of Jeffrey A. Whitsett), TTF-1 (M3575, 1:100; DakoCytomation, Hamburg, Germany), vimentin (C-20, 1:200; Santa Cruz Biotechnology), E-cadherin (clone ECCD2, 1:250; Zymed Laboratories), E-cadherin (clone 24E10, 1:250; Cell Signaling Technology), phospho-Akt (4060, 1:50; Cell Signaling Technology), phospho-ERK (4376, 1:100; Cell Signaling Technology), active β-catenin (clone 8E7, 1:100; Millipore, Schwalbach, Germany), myc tag (9E10, 1:100; Santa Cruz Biotechnology), acetylated tubulin (T7451, 1:5000; Sigma), PGP 9.5 (7863-0504, 1:5000; AbD Serotec), β-catenin (06-734, 1:100; Upstate Biotechnology, Lake Placid, NY). Following primary antibody incubation, sections were incubated with the corresponding biotinylated secondary antibodies (DakoCytomation) at a 1:200 dilution for 60 minutes at room temperature. ABC reagent was applied (Vectastain Elite ABX Kit; Vector Laboratories, Burlingame, CA) and developed in DAB. Sections were then counterstained with hematoxylin and mounted after dehydration. Phospho-p44/p42 mitogen-activated protein kinase (MAPK) staining was essentially carried out as the others except that TBS with 1% Tween 20 was used instead of PBS. CCSP and pro SpC dual immunofluorescence staining was done as previously described [5]. For immunofluorescence staining, the following secondary antibodies (all obtained from Jackson Immuno-Research Laboratories, West Grove, PA, at 1:200 dilutions) were used: donkey anti-mouse Cy3, donkey anti-mouse Cy5, donkey anti-goat Cy5, donkey anti-goat Cy3, donkey anti-rabbit Cy3, donkey anti-rabbit Cy5, donkey anti-rabbit Alexa 488, donkey anti-rat Cy3, donkey anti-rat Cy5. For Alcian Blue staining, lung sections were deparaffinized, rehydrated in graded series of alcohols, and incubated in Alcian Blue (pH 2.5, Sigma) solution for 30 minutes at room temperature. After washing in tap water for 5 minutes, sections were counterstained with Nuclear Fast Red (Sigma) for 5 minutes, washed with tap water for 3 minutes, dehydrated, and mounted with Entellan. For microscopy, we employed the Zeiss Axio Scope.A1 or the Zeiss Discovery.V8 Stereo microscopes (Carl Zeiss MicroImaging GmbH) integrated with an AxioCam ICc3 camera (Spectra Service). Images were acquired using AxioVision Rel. 4.7 software provided by Zeiss. Negative controls included the omission of the primary antibody.

Morphometric Analysis

Quantitation of ciliated cells was assessed by determining the length of basement membrane underlying tubulin$^+$ regions of the epithelium and dividing this value by the total length of the basement membrane. Ciliated cells were scored from at least 10 bronchioles per lung. At least four mice for each group were counted. Epithelial repair was quantified at day 2 and day 18 recovery time points by determining the length of basement membrane underlying CYP2F2$^+$ or CCSP$^+$ regions of the epithelium and dividing this value by the total length of the basement membrane. The length of the bronchial epithelium was determined using the measurement function of Zeiss Axio Scope.A1. For quantitative assessment of NEB-associated PNECs or Clara^V cell proliferation, triple immunofluorescence staining was performed on lung sections using CGRP, CCSP, and Ki-67 antibodies. Clara^V cells were identified with their association with CGRP-expressing neighboring NE cells.

Naphthalene Exposure

Five-week-old male compound (*CCSP rtTA/Tet-O dn E-cadherin*) mice were intraperitoneally injected with 250 mg/kg body weight of naphthalene (Sigma) dissolved in corn oil. Animals were sacrificed 2 or 18 days following naphthalene or corn oil treatments.

BASC Sorting by Flow Cytometry

BASCs were isolated from the lungs of 6-week-old DTR mice according to established protocols [6]. Briefly, mice were sacrificed, and their lungs were removed and cut into small pieces. Tissue dissociation was performed by treating with Dispase (Invitrogen) at room temperature for 60 minutes, then passing the lungs through 100-, 70-, and 40-μM filters to obtain a single-cell suspension. After washing with PBS, cells were stained with phycoerythrin (PE)-conjugated anti-CD45 and anti-CD31 (eBioscience, San Diego, CA), fluorescein isothiocyanate–conjugated anti-CD34, and subsequently with PE-CY5–conjugated anti-Sca1. After a 30-minute incubation, cells were washed three times and sorted using fluorescence-activated cell sorting (FACS). Flow cytometric analysis was performed on a FACSCalibur (BD Immunocytometry Systems) according to the manufacturer's instructions.

Statistical Analysis

All statistical analyses were performed using GraphPad Prism 5 software (GraphPad Software, Inc). Student's t test (two-tailed) was used to compare two groups. When more than two groups were compared, differences among the groups were determined by one-way analysis of variance. Differences between means were considered statistically significant when $P < .05$.

Supplementary References

[1] Dahl U, Sjodin A, and Semb H (1996). Cadherins regulate aggregation of pancreatic β-cells *in vivo*. *Development* **122**, 2895–2902.

[2] Liu C, Glasser SW, Wan H, and Whitsett JA (2002). GATA-6 and thyroid transcription factor-1 directly interact and regulate surfactant protein-C gene expression. *J Biol Chem* **277**, 4519–4525.

[3] Van Winkle LS, Gunderson AD, Shimizu JA, Baker GL, and Brown CD (2002). Gender differences in naphthalene metabolism and naphthalene-induced acute lung injury. *Am J Physiol Lung Cell Mol Physiol* **282**, L1122–L1134.

[4] Wu CA, Peluso JJ, Shanley JD, Puddington L, and Thrall RS (2008). Murine cytomegalovirus influences Foxj1 expression, ciliogenesis, and mucus plugging in mice with allergic airway disease. *Am J Pathol* **172**, 714–724.

[5] Rapp UR, Korn C, Ceteci F, Karreman C, Luetkenhaus K, Serafin V, Zanucco E, Castro I, and Potapenko T (2009). MYC is a metastasis gene for non-small-cell lung cancer. *PLoS One* **4**, e6029.

[6] Kim CF, Jackson EL, Woolfenden AE, Lawrence S, Babar I, Vogel S, Crowley D, Bronson RT, and Jacks T (2005). Identification of bronchioalveolar stem cells in normal lung and lung cancer. *Cell* **121**, 823–835.
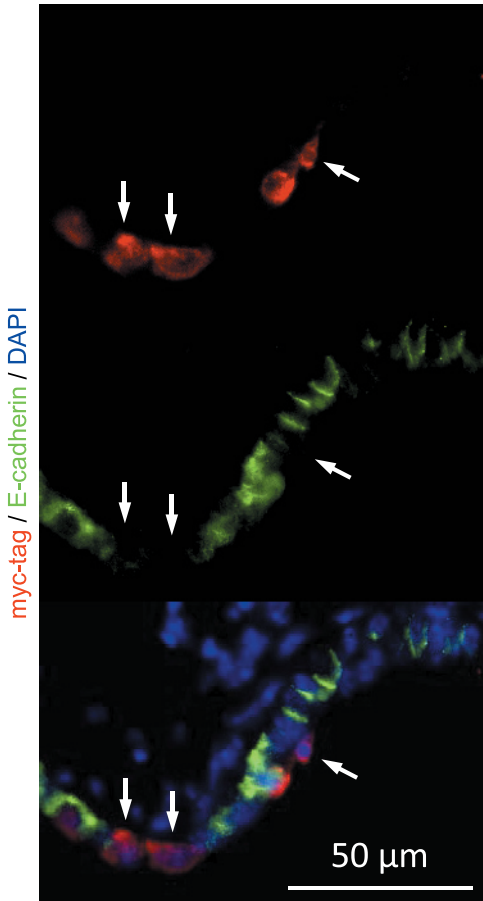
Figure W1. Analysis of subcellular distribution of endogenous E-cadherin in conducting airway cells after dn E-cadherin expression. Representative dual immunofluorescence staining of lung sections from induced DTR mice for myc tag (red) and E-cadherin (green). Images are representative of $n = 3$ separate mice per treatment group. Arrows indicate myc tag–expressing cells that are negative for E-cadherin. Nuclei were counterstained with DAPI (blue).
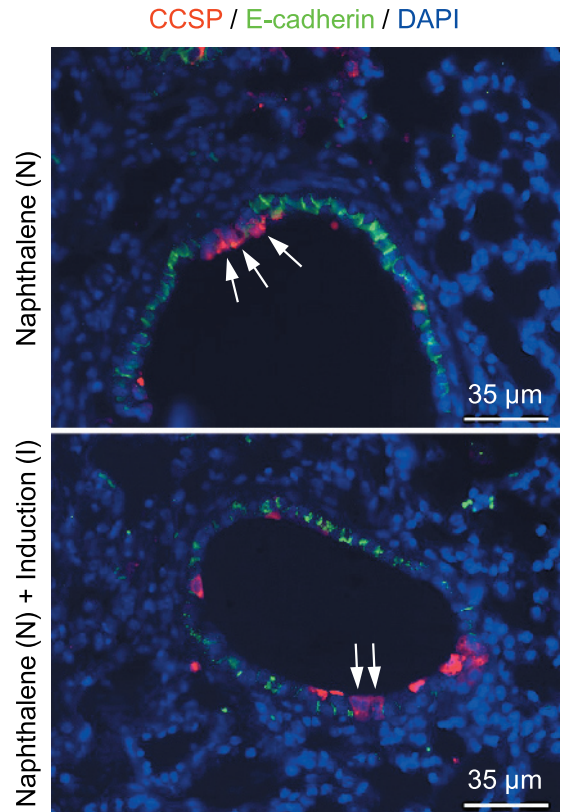

Figure W2. Analysis of CCSP and E-cadherin expression in conducting airways after naphthalene treatment. Dual immunofluorescence staining of lung sections for CCSP (red) and E-cadherin (green). Images are representative of $n = 3$ separate mice per treatment group. Five-week-old mice were treated as indicated. Mice were recovered following 2 days from naphthalene exposure. Arrows indicate naphthalene-resistant Clara cells.
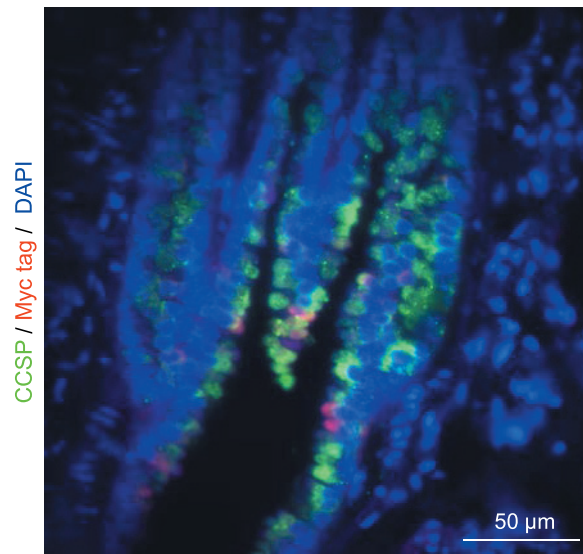
Figure W3. Analysis of the transgene expression in induced hyperplastic lesions. Double immunofluorescence staining of a representative lung section from an induced mouse for the indicated markers shows that only minority of the hyperplastic cells express the transgene.
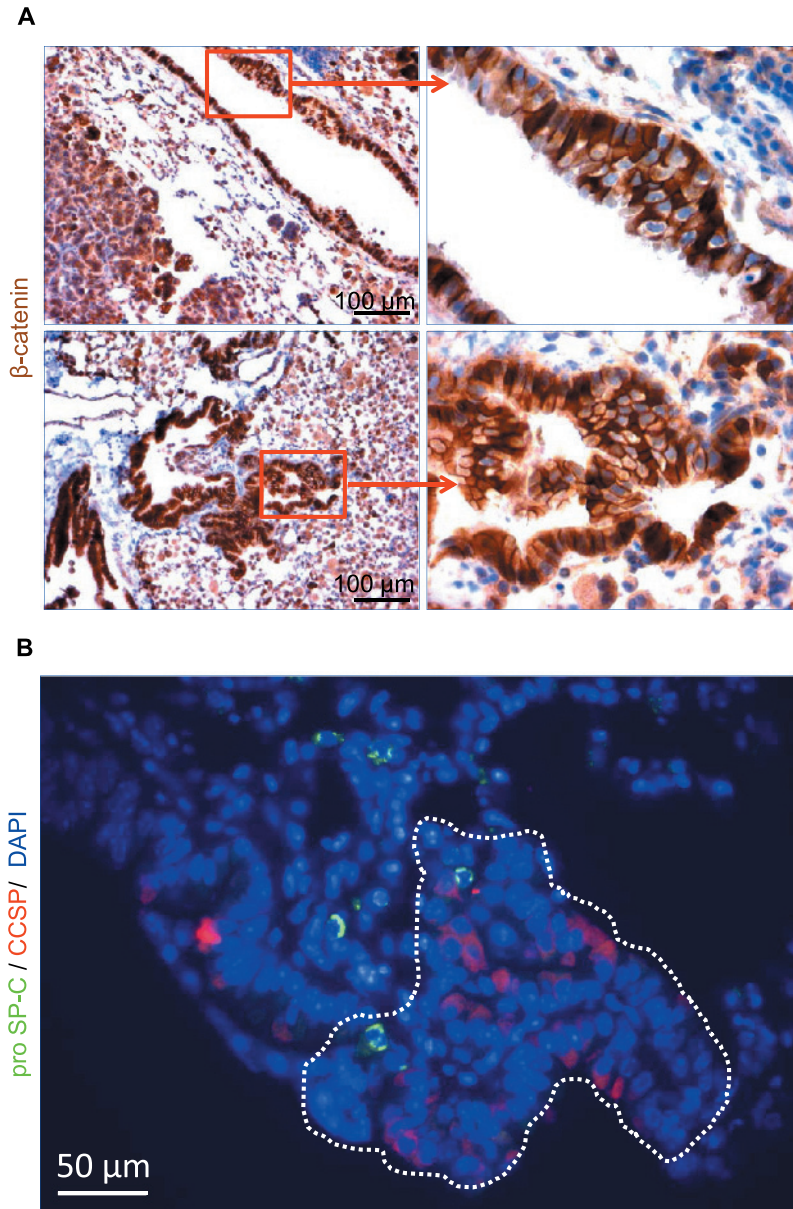
Figure W4. (A) β-Catenin immunohistochemistry and analysis of abundance of alveolar type II cells in the hyperplasia. (A) Paraffin-embedded lung sections from induced DTR mice stained for β-catenin (brown). Right panel pictures are the high magnification of the insets. Hematoxylin (blue) was used as a counterstain. (B) Double immunofluorescence staining of a representative hyperplastic lesion for CCSP (red) and pro SpC (green) shows that most of the cells in the hyperplasia are negative for pro SpC. Nuclei were counterstained with DAPI (blue). Dotted lines outline the hyperplastic area.
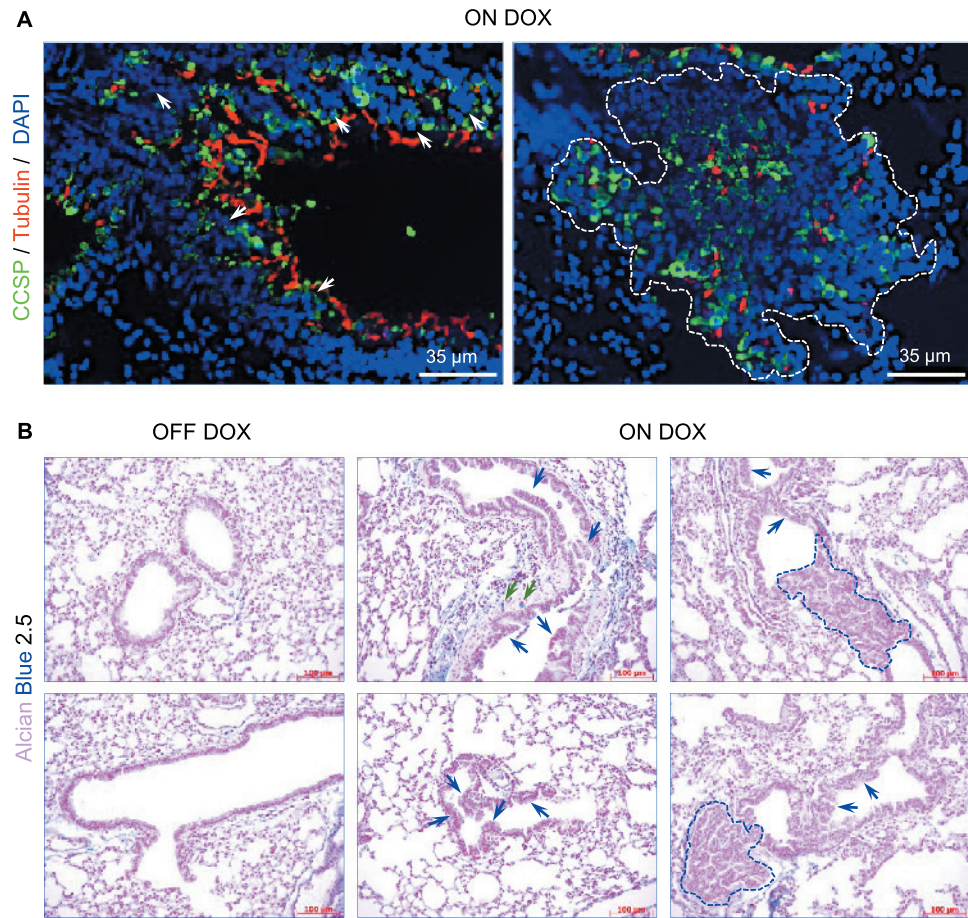
Figure W5. Analysis of abundance of ciliated and goblet cells in induced bronchiolar hyperplasia. (A) Double immunofluorescence staining of lung sections from induced mice for indicated markers. Nuclei were counterstained with DAPI (blue). White arrows and the marked region show early and progressive bronchiolar hyperplasia, respectively. (B) Alcian Blue 2.5 staining of lung sections from control (OFF DOX) and induced (ON DOX) mice. Green arrows show Alcian Blue–positive goblet cells. Blue arrows and the marked regions show early and progressive bronchiolar hyperplasias, respectively.
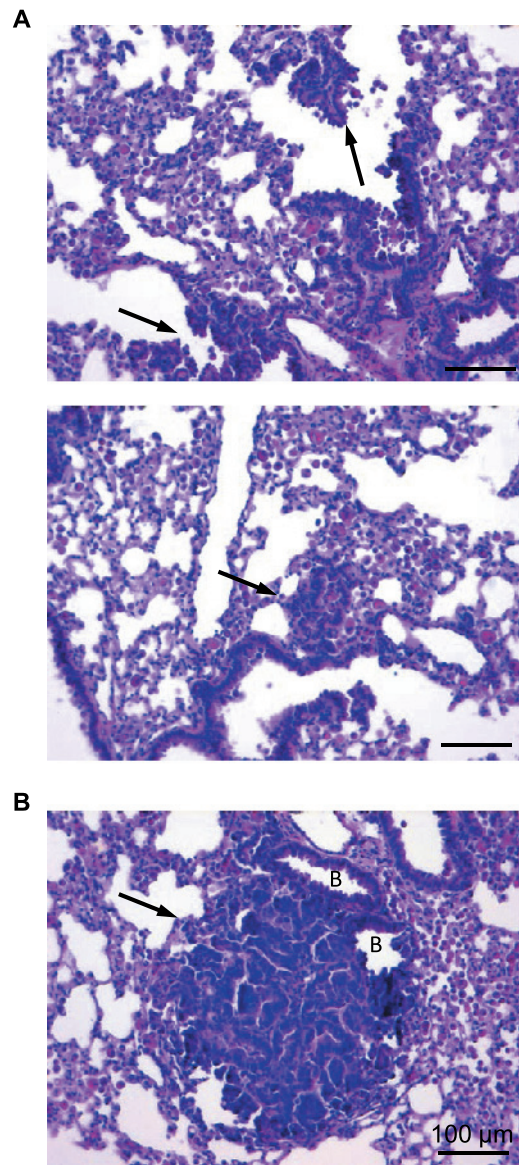
Figure W6. Early lung tumors in induced DTR mice resemble the papillary hyperplastic lesions and are associated with conducting airways. (A) Histologic analysis through H&E staining of lungs from DOX-treated DTR mice showing the epithelial hyperplasia (arrows). (B) H&E staining of a lung section from a 7-month DOX-treated mouse shows a budding lung tumor (arrow) from a bronchiole.
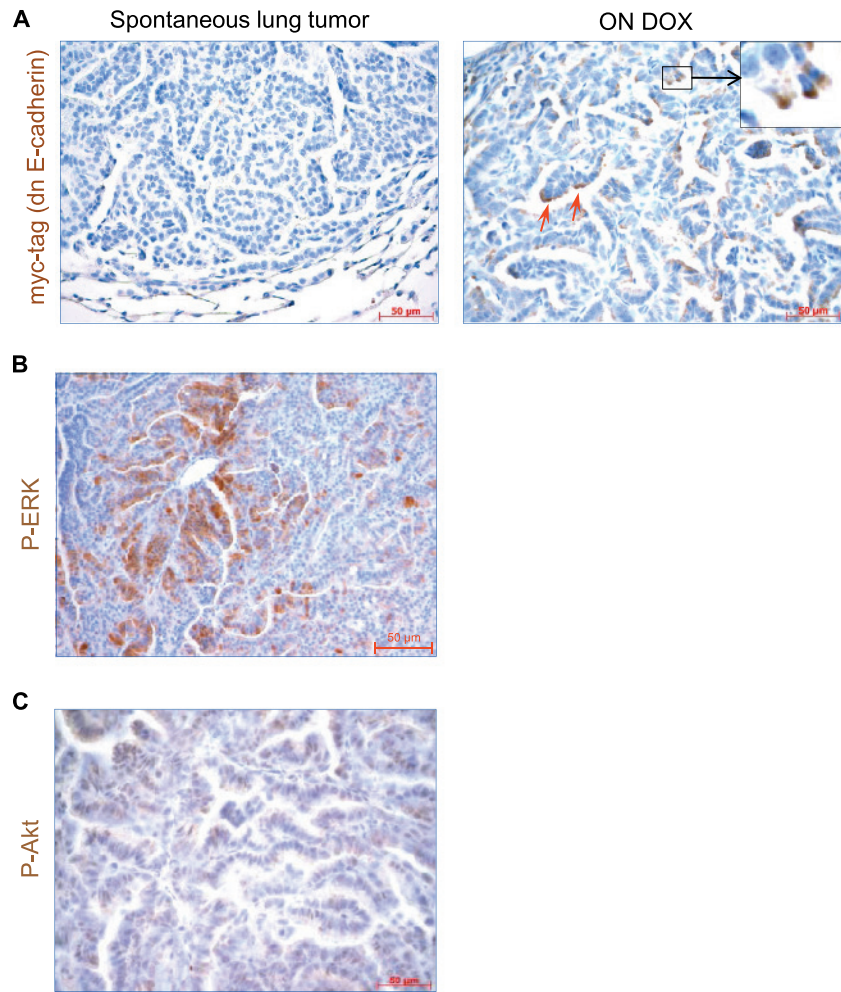
Figure W7. Analysis of transgene, phospho-ERK, and phospho-Akt expression in induced lung tumors. (A) To distinguish spontaneous lung tumors from induced tumors, we performed immunohistochemistry for myc tag on lung sections. Red arrows show myc tag–expressing rare tumor cells in an induced lung tumor. Note the absence of myc tag staining in the spontaneous lung tumor. High-magnification image represents the region shown in the inset. Hematoxylin (blue) was used as a counterstain. Immunohistochemistry of lung tumor sections from a 10-month-old mouse for pERK (B) and for pAkt (C). Hematoxylin (blue) was used as a counterstain.
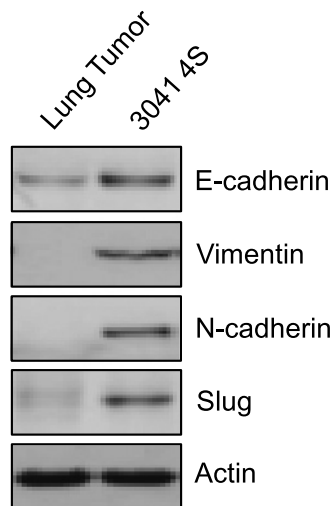
Figure W8. Lack of EMT-associated markers in induced lung tumors. Western blot analysis of a lung tumor from an induced mouse was probed against the indicated markers for evaluation of EMT activation. A mouse NSCLC cell line (3041) transfected with a stabilized form of β-catenin (4S) was used as positive control for the markers.